

This is a pre print version of the following article:

Interactions between elastin-like peptides and an insulating poly(ortho-aminophenol) membrane investigated by AFM and XPS / Carbone, Maria Elvira; Ciriello, Rosanna; Moscarelli, Pasquale; Boraldi, Federica; Bianco, Giuliana; Guerrieri, Antonio; Bochicchio, Brigida; Pepe, Antonietta; Quaglino, Daniela; Salvi, Anna Maria. - In: ANALYTICAL AND BIOANALYTICAL CHEMISTRY. - ISSN 1618-2642. - 410:20(2018), pp. 4925-4941. [10.1007/s00216-018-1142-3]

Terms of use:

The terms and conditions for the reuse of this version of the manuscript are specified in the publishing policy. For all terms of use and more information see the publisher's website.

18/12/2025 03:46

Interactions between elastin-like peptides (ELPs) and insulating poly ortho-aminophenol (PoAP) membrane investigated by AFM and XPS

Maria Elvira Carbone^{1*}, Rosanna Ciriello¹, Pasquale Moscarelli², Federica Boraldi², Giuliana Bianco¹, Antonio Guerrieri¹, Brigida Bochicchio¹, Antonietta Pepe¹, Daniela Quaglino², Anna Maria Salvi^{1*}

¹Università degli Studi della Basilicata, Dipartimento di Scienze, DiS, Viale dell'Ateneo Lucano 10, 85100 Potenza, Italy

² Università degli Studi di Modena e Reggio Emilia, Dipartimento di Scienze della Vita, Via Campi 287, 41125 Modena, Italy

*Authors to whom correspondence should be addressed:

✉ anna.salvi@unibas.it

✉ maria.carbone@unibas.it

Abstract

The present investigation was undertaken to explore the mutual recognition of the pentapeptide (ValGlyGlyValGly)_n, a hydrophobic elastin-like peptide (ELP), suspended in deionized water in monomer (n=1) and trimer (n=3) forms, and the outer surface of a very thin, insulating polymer, PoAP, electrochemically grown on a platinum foil by Cyclic Voltammetry, CV, in neutral media (PBS, I=0.1M), immersed in the suspension.

As a prior task, the proved propensity of the ValGlyGlyValGly sequence, at the given minimal length (n-repeats ≥ 3), to self-assembly into amyloid-like fibrils when solubilized in aqueous environment, was here considered in the prospect of testing PoAP surfaces for the specific detection of amyloid precursors.

Based on our knowledge of chemical structure and physical properties of both bio-macromolecule families, gained in previous studies, we have focused our attention on the efficacy of binding sites offered to ELP fibrils by PoAP in its 'as prepared' form or properly modified either by post-synthesis oxidation and by adsorption/entrapping of ELP monomer(s) with or without 'protecting' terminal groups.

Consistently with all ways of preparation, the best surfaces, recognizable by the trimer fibrils, are those modified to carry a larger number of carbonyls, particularly, by entrapment of ELP monomer(s) during PoAP electro-synthesis, using an imprinting- inspired methodology.

The degree of attachment of fibrillar aggregates, detected by AFM and XPS techniques, provide unequivocal evidence of the cooperative forces involving PoAP-ELPs interactions. Interesting results have emerged all converging in the perspective of qualifying the proposed Pt/PoAP/ELP systems as bio-detectors to improve diagnostic exploitation in Alzheimer Disease.

Keywords

XPS, AFM, Poly ortho-Amino Phenol (PoAP), Elastin-like peptides (ELPs), Amyloids, Peptides-imprinted CV-polymerization

INTRODUCTION

One important marker of Alzheimer’s disease (AD) is the deposition and accumulation of amyloid (A β) fibrils into insoluble plaques being associated to age-dependent cognitive changes and dementia [1-8]. The A β peptides, generated by the amyloidogenic cleavage of Amyloid Precursor Protein (APP) [5,6, 9-11], are highly predisposed to self-aggregate and to transform, rapidly, if over-produced, into β -stranded oligomers and proto-fibrils finally evolving into amyloids accumulating around neurons. It is widely recognized that of these A β variants, soluble monomers/oligomers are the most abundant forms in preclinical stages, while their level drops with disease onset and progression due to their sinking into amyloid plaques. It is thus of great importance the development of biosensors for the specific determination of amyloid-beta peptides and their aggregates, considering either early and late stage detection as well as total A β variants. As recently reported [5, 12-19], in addition to the very few protocols already approved for clinical diagnosis, multi detection systems based on aptamers and molecularly imprinted polymers working in body fluids other than CSF are expected to emerge in the near future.

In particular, among the currently proposed biosensors, those holding adsorbed or ‘imprinted’ receptors are used to an increasing extent for selectively monitoring peptides and proteins. Therefore, the ‘anchoring’ of hydrophobic and strongly self-aggregating amyloid peptides represent new challenge in the diagnostics of amyloid precursors [19-24].

As a natural evolution of the research work dedicated by our group to the synthesis and characterization of nanostructured biopolymers and to their bio-analytical applications, the present contribution proposes a model system based on the conjugated action of polymers and peptides as an analytical tool for a deeper understanding of the mutual interactions of amyloidogenic peptides, to improve their diagnostic exploitation.

Within this context, we recall the *CV* electro-synthesis of ortho-aminophenol (oAP), a very interesting organic compound due to its ability to form conductive or insulating polymers, PoAP, under electrochemical oxidation in acidic and neutral/basic media, respectively [25-29]. Moreover, we have synthesized, as innovative compounds, self-assembling hydrophobic elastin-like polypeptides (ELPs), of the general type (XxxGlyGlyZzzGly)_n (Xxx, Zzz=Val, Leu), that have been extensively characterized [30-34], and tested for biocompatibility with mouse 3T3 fibroblasts [35,36].

Among PoAP and ELP samples, we have in turn selected insulating PoAP and the ELP sequence ValGlyGlyValGly (reported hereinafter as VGGVG), as the most suitable compounds for the present application.

Briefly, insulating PoAP was revealed by AFM investigation to be a homogeneous membrane, fully adhering to the underneath platinum, easy to handle, with a constant repeat formula, as derived by XPS, made of alternating quinoneimine and oAP units and water molecules firmly retained within the polymer structure. Reproducibility tests have shown PoAP to be highly stable even under ultra high vacuum (UHV); thus, most likely, strong H-bonds occur along the polymer chains, perhaps necessary for PoAP alignment. We could extrapolate that, sustained by water molecules, the short PoAP chains (estimated 10 nm, on average) are aligned vertically, ending with imino groups progressively transforming to 'carbonyls' by post-synthesis oxidation in air [25,27, 37,38].

The ELP sequence (VGGVG)_n was selected due to its high propensity to self-assemble in amyloid-like fibrils when suspended in water at a given length ($n \geq 3$) [32,35,36] and being already studied in variable repeat forms, solvent choices and operative conditions: as a monomer ($n=1$) with and without protecting hindering terminal groups, as a trimer ($n=3$) and as a log-normal dispersed polymer chains (with the degree of polymerization, n , centered on 5). Modeling of the water-induced self-assembly was also attempted for poly (VGGVG) in comparison with the homologue poly (LGGVG) [31] based on the cooperative reinforcement of carbonyls H-bonds and hydrophobic interactions by aliphatic chains of their extended β -sheet structures, revealed by FTIR studies. Thus, to the specific aim of providing suitable bio-receptors for amyloids and their precursors, knowing that all amyloid fibrils share a common self-assembly pathway and final β -pleated sheet structure [39-42], these amyloidogenic elastin-like peptides were sought to reproduce, properly, the molecular events of A β variants as indicators of AD biomarkers.

Based on the two branches of results, we have then planned experiments in the order herein reported, following the procedures listed in the experimental section:

- a) XPS and AFM studies of VGGVG pentapeptides and (VGGVG)₃ pentadecapeptide (trimer) deposited on silicon substrate from water suspensions, as integrative of previous investigation on ELPs self-assembly [30-34], carried under identical modalities;
- b) Study of the direct interaction between insulating PoAP, freshly prepared or stored in air for days before use, and (VGGVG)₃ trimer, long aged in deionized water;

- c) Study of PoAP and (VGGVG)₃ interactions, mediated by VGGVG monomers pre-adsorbed on PoAP surfaces from water solutions, differently aged at ambient conditions, monitoring the influence of VGGVG terminal groups.
- d) Study of PoAP and (VGGVG)₃ interactions, mediated by VGGVG monomers entrapped at or near the PoAP surface, during CV electro-synthesis, finding inspiration on Molecularly Imprinted Polymer (MIP) technology [43-45], more precisely, on bi-dimensional MIP [46] given the ultrathin thickness of PoAP membrane adhering on platinum, estimated to be less than 10nm [25-27, 37,38]

Regarding PoAP, we have focused our attention on the binding propensity of the outermost carbonyls, and on their concentration and efficacy as a function of the storage time.

Regarding ELP sequences, we have given the priority to both unprotected and terminal-protected VGGVG monomers, i.e. to the pentapeptide unity, known to be too short in length for evolving as amyloid fibrils, likely suitable to be used as surface receptors for the trimer fibrils, if properly adsorbed/entrapped on PoAP. Previous studies have amply demonstrated that amyloid fibrils formed by (VGGVG)₃ are much smaller and more homogeneously distributed when deposited on substrates, compared to those formed by poly(VGGVG) [30-34]. The minor tendency to associate and entangle with each other leaves the trimer, at the concentration (0.1mg/mL) used in this work, to self-assembly in a kind of pre-fibrillar state: therefore, the old-aged (VGGVG)₃ suspension, available from previous experiments [35,36] was considered suitable for our scope.

Regarding the layered Pt/PoAP/ELP systems, attention was posed on the action of VGGVG monomers as surface bio-detectors, exploiting two methods for their immobilization onto the polymeric film, by surface adsorption and by physical entrapping in the same manner as usually done for the two-dimensional MIP. It is known, indeed, that these peptide sequences tend to spontaneously identify similar repetition units, making then a more complex structure, the repeated extended β -sheet, by the formation of inter-chain hydrogen bonds, reinforced by hydrophobic interactions [30,39,40].

In order to understand their assembly and their performance as amyloids detectors, the systems were all tested by XPS and AFM, before and after immersion in the aged suspension of trimer fibrils, also considering the influence of the underneath platinum.

MATERIALS AND METHODS

Chemicals

The monomer of ortho-aminophenol, oAP, (Fluka, purity 99%, FW = 109.13 g/mol) was purified, before being used, by recrystallization in ethyl acetate (Sigma Aldrich, purity 99%, d = 0.9 g/mL, bp = 76.5 °C) and with activated carbon, as suggested by Ortega [47]. Monomer oAP solutions were prepared in supporting electrolyte just before their use. The procedures for the synthesis of unprotected VGGVG and Boc-VGGVG-OEt pentapeptides and for the pentadecapeptide (VGGVG)₃ are reported in details in previous studies [34-36, 48]. Pure water supplied by Milli-Q RG unit from Millipore (Bedford, MA, USA) was used throughout. All other chemicals were of analytical grade and were used without further purification.

Experimental setup

Electrochemical apparatus and film deposition

Electrochemical experiments were carried out with an EG&G PAR model 263A potentiostat/galvanostat. Data acquisition and potentiostat control were accomplished with a desktop computer running the M270 Electrochemical Research Software (EG&G), version 4.23. All experiments were carried out at room temperature in a standard three-electrode cell employing an Ag/AgCl/KCl (sat) reference electrode and a platinum counter electrode. The working electrode was a platinum foil (10×15×0.127mm, 99.99%, Aldrich). No action was taken to remove oxygen from solutions. Platinum working electrodes were cleaned following the reported procedure [27]. The insulating PoAP film was electrosynthesized by cyclic voltammetry, scanning the electrode potential for 20 cycles between -0.1 and +0.9 V (vs. Ag/AgCl, saturated KCl) in a 5 mM oAP solution in phosphate buffer (I=0.1 M, pH 7) at a scan rate of 50 mV/s.

All the electrochemically synthesized PoAP films were then washed with double-distilled water and dried at room temperature in nitrogen atmosphere before their ex-situ analyses or further manipulations.

ELPs absorption onto PoAP/Pt electrodes

The PoAP/Pt modified electrodes were dipped into ELPs (VGGVG or Boc-VGGVG-OEt) solution, 0.1 mg/mL, for 6 hours at 37°C, subsequently rinsed with Milli-Q water and left to dry overnight before proceeding with AFM and XPS analyses.

All the Pt/PoAP/ELP electrodes were then washed with double-distilled water and dried at room temperature in nitrogen atmosphere before their ex-situ analyses or further manipulations.

ELPs entrapment onto PoAP/Pt electrodes

The modified Pt/PoAP/ELP electrode was obtained by cyclic voltammetry (CV), scanning the electrode potential for just one cycle between -0.1 and +0.9 V (vs. Ag/AgCl, saturated KCl) in a 5 mM oAP solution in phosphate buffer (I=0.1 M, pH 7) at a scan rate of 50 mV/s. After the addition of 500 μ L of the 0.1 mg/mL VGGVG (or Boc-VGGVG-OEt) solution to the supporting electrolyte (8 mL), the PoAP electropolymerization has been prolonged for other 19 voltammetric scans.

In order to check the sensing capabilities of these systems, the modified electrodes were dipped into (VGGVG)₃ suspension for 6 hours at 37°C, subsequently rinsed with Milli-Q water and left to dry overnight before proceeding with AFM and XPS analyses.

XPS measurements

XPS analysis were performed by a Phoibos 100-MCD5 spectrometer, operating in Medium Area lens mode (spot of $\varnothing = 2$ mm, entrance slit of 7x20 mm). Spectra were acquired with achromatic Al K α radiation (1486.6 eV) operating at 10 kV and 10 mA. The pressure in the analysis chamber was typically about 10^{-9} mbar during acquisition. A pass energy of 9 eV was used to collect the wide and the detailed spectra, using fixed analyzer transmission (FAT) operation mode with channel widths of 1.0 and 0.1 eV, respectively. All XP spectra were acquired at a 90° take-off angle. The energy scale of the spectrometer was calibrated with Cu2p_{3/2} (932,7 eV) and Au4f_{7/2} (84,0 eV) signals using pure metals (Johnson Matthey) for spectroscopic analysis.

Curve-fitting procedure

The XPS spectra were analysed using a curve-fitting program “Googly” which gives to each individual peak its own intrinsic Shirley-like background and extrinsic tail, as fully described in previous works [49,50]. Peak areas were converted to atomic composition using established procedures and the appropriate sensitivity factors, SF [39]. The criteria adopted for data elaboration were based on preliminary analyses of reference compounds and literature data, also available online [51], to assure the correct sample stoichiometry, in the limit of XPS accuracy [52,53].

The energy scales of the detailed regions are converted to binding energy so as to facilitate comparison of the curve fitted results with literature data and the peak assignments, reported in the relevant tables, are corrected for surface charging by referring to C1s aromatic carbon, used as an internal standard and set at 284.8 eV.

AFM analysis

AFM images were carried out by using the XE-120 microscope (Park Systems) in air and at room temperature. Data acquisition was carried out in non-contact mode at scan rates between 0.15 and 2.20 Hz, using rectangular Si cantilevers (NCHR, Park Systems, tip radius less than 5 nm) with the nominal resonance frequency and force constant of 330 kHz and 42 N/m, respectively.

RESULTS AND DISCUSSION

a) XPS and AFM analyses of reference bio-macromolecules

AFM images and XPS curve-fitted spectra of three ELPs, H₂-VGGVG-OH, Boc-VGGVG-OEt and (VGGVG)₃ deposited on silicon wafer from water suspension are shown in Figures 1 and 2. XPS curve-fitting results of Figure 2 are summarized in Table 1.

These surface analyses complement those related to protected Boc-VGGVG-OEt characterized in the solid state [34] and insulating PoAP, fully characterized in previous works [25-27, 37,38], allowing a more comprehensive interpretation of data.

For instance, the secondary structures of unprotected H₂-VGGVG-OH were already assigned by circular dichroism (CD) and nuclear magnetic resonance (NMR) investigations [54] and interpreted as an incipient tendency of this pentapeptide to ‘head to tail’ interactions, when it is present in pure water in the ionized H₃⁺-VGGVG-O⁻ state. Present data support previous observations demonstrating that deposits from water suspension show a more ordered aggregation compared to its protected homologous (see also supplementary materials).

Moreover, previous XPS analyses on powdered Boc-VGGVG-OEt revealed intra-chain C=O...H-N< bonds responsible for the folded secondary structure of this terminal-protected pentapeptide [34]. Similar XPS results and globular (amorphous) aggregation were obtained investigating peptide deposits on silicon from water suspension, as reported in Figures 1b, 2b.

Regarding the amyloidogenic (VGGVG)₃ (Figures 1c, 2c), XPS reveals the carbonyl splitting due to the action of bridging water, associated to amyloid fibrils as reported for poly VGGVG [30-31, 34]. AFM images unequivocally show the presence of amyloid-like fibrils, shorter and thinner with respect to those formed by poly VGGVG [30,31] and more homogeneously distributed (coexisting with pre-fibrillar aggregates of regular morphology).

The morphology of the polymer PoAP [25,27], instead, is totally deprived of structures. As already shown, insulating PoAP is reproducibly electro-synthesized by CV, in neutral media, with an average thickness of about 10 nm, as estimated by both AFM and XPS, as a thin film perfectly adhering to the platinum substrate. Its growth is self-limited by the fast current decay when the

substrate coverage is complete. The curve-fitting of XPS spectra, acquired at different take-off angles, gives highly reproducible results concerning the chemical formula derived as repeat unit, the presence of water within the polymer chains and of carbonyls on the outermost layers, increasing with time by post-synthesis oxidation of terminal C=N groups [26].

Based on previously reported PoAP specificities and indications on ELPs self-assembly, the use of the insulating PoAP-ELPs system, for each combination shown in the following paragraphs, was designed to deepen the understanding of the aggregation phenomena underlying the incipient formation of amyloids, using XPS and AFM as combined means of investigation. Results of XPS curve-fitted spectra, selected as appropriate and indicative of all experiments performed, are cited along the text and summarized in [Table 2](#).

b) Study of the direct interaction of insulating PoAP, freshly prepared or stored in air for days before use, and (VGGVG)₃ aged in deionized water.

To perform this study, insulating PoAP was first electro-synthesized by CV on platinum, as previously defined, then the rinsed rectangular shaped Pt/PoAP electrode was immersed in a long aged (VGGVG)₃ suspension for 6 hours at 37°C, using the same interaction time and temperature of previous investigation on 3T3 fibroblasts' adhesion onto ELPs-coated surfaces [35,36].

Figures 3 compare the magnified AFM images and C1s spectra of Pt/PoAP before and after the exposure to (VGGVG)₃ suspension. It is clearly evident that both analyses reveal little interaction between (VGGVG)₃ and freshly prepared PoAP although XPS seems to indicate, by the change of the C1s peak shape, the adsorption of very thin layers not distinguishable by AFM from the substrates' morphologies.

However, knowing the steady increase of carbonyls on PoAP surface due to oxidation of C=N groups in air, the same experiment was repeated using the Pt/PoAP electrode left in ambient conditions for 15 days, after preparation. Figures 4 and Table 2 clearly show different results at this time point. The AFM image (4d) reveals the presence of aggregates, referable to trimer pseudo-fibrils, locally massed on the aged PoAP surface. XPS curve-fitted spectra (4a-c), difficult to accurately quantify because of the uneven morphology/topography, qualitatively confirms the appearance of additional signals, if compared to the curve-fitted C1s, O1s and N1s regions of the "as prepared" PoAP [25, 26], clearly related to trimer adsorption on PoAP. Focusing on C1s, the most significant XPS region, we can identify these signals, being labeled in Figure 4a, but absent in both the C1s spectra of Figures 5, related to Pt/PoAP surfaces, differently aged, before immersion

into (VGGVG)₃ suspension. Indeed, C1s spectra of freshly prepared, Figure 5a, and in air-stored, Figure 5b, PoAP, show the same chemical groups and differences in peak shapes due to the increase of carbonyl contents, passing from 7.0 to 10.6 At%, respectively, as derived from Table 2.

Thus, the effect of air oxidation on the external groups seems quite beneficial for our purposes. Since the increase of carbonyl amount causes a greater trimer adsorption on PoAP, it can be supposed that their interaction is mediated by PoAP carbonyls, as terminal functionalities, likely through H-bonds with the ELPs NH-C=O peptide groups, the same inter-chain bonds of amyloid peptides. The surface reconstruction of PoAP due to ageing, influencing its activity towards fibrils adsorption, cannot be disregarded a priori, however, topographical/conformational changes are hardly discernable in AFM images of Figures 4c,d related to fresh and aged PoAP, respectively.

Therefore, we can only assume that carbonyls present on the outermost surface, attributed to a *posteriori* oxidation of imino groups, are numerically inadequate on freshly prepared PoAP to bond (VGGVG)₃ efficiently, while, the prolonged PoAP storage in air increases their abundance allowing a better anchoring along the trimer sequence.

However, this method is time-requiring and storing conditions could be difficult for PoAP to be reproduced. Therefore, in order to functionalize in a more systematic way our Pt/PoAP electrode, we tried to pre-adsorb on it the shorter peptide sequence, VGGVG. It was expected that the right monomer(s) coverage would facilitate a more copious and homogeneous (VGGVG)₃ adsorption on PoAP, having the same functional groups and the same amino acid sequence of its repeat.

c) Study of PoAP and (VGGVG)₃ interactions mediated by VGGVG monomers pre-adsorbed on PoAP surfaces from water solutions, differently aged, in air at room temperature

To pre-adsorb VGGVG monomers on Pt/PoAP surface the procedure adopted for the trimer detection was used, as reported in the experimental section.

Since we have demonstrated that unprotected and terminal-protected VGGVG monomers differently self-aggregate in water (Figures 1-2), to verify if these different morphologies slowly evolve with time and to find the conditions for achieving the best PoAP-ELPs interaction, we have performed a set of experiments, using three different aging times for both monomer types, (see 'Supplementary Materials' comprehensive of S1-S5 Figures).

Results lead to important outcomes on the use of Pt/PoAP/ELP for trimer detection.

In particular, the unprotected pentapeptide adsorbs on PoAP mainly via H-bonds involving carbonyls of either side, therefore, fresh adsorption leaves the prominent aliphatic component, likely resulting by side chains exposed outward, preventing further adhesion. A suitable ageing time was required for the monomer sequence to elongate, most likely via head to tail interaction, to a point that a proper number of carbonyls could be left unbounded on PoAP surface and exposed outwards for the subsequent detection of the trimer fibrils. The implicit, collateral, discovery was that monomer sequences, too short to self-assemble into amyloids, can still aggregate into unexpected supra-molecular features, with time and by external inducers as the external surface of Pt/PoAP electrode, immersed in the monomer solutions (Figure S1).

The terminal protected pentapeptide adsorbs on PoAP mainly via hydrophobic forces, involving ELP' aliphatic side chains and PoAP' aromatic moieties, therefore, free carbonyls were mostly available outward, without any need to age the monomer solution. Therefore, the influence of time on self-aggregation was not further investigated. However, the 'progressive coverage' of PoAP (decreasing Pt/N ratio) was found to correlate with the 'ageing' time of the monomer' solution (Figure S3).

The adsorption method has provided precious information on the polymer-peptide interaction, on their ability of mutual recognition, either via H-bonds between interfacing carbonyls and hydrophobic forces involving ELP' aliphatic side chains and PoAP' aromatic moieties. These forces are exactly the same as those driving the self-assembly of hydrophobic peptides of the type (XxxGlyGlyZzzGly) (Xxx,Zzz= Val, Leu), into extended β -sheet amyloids [30,39,40]. In particular, carbonyls as ending groups and aromatic moieties of PoAP chains appear to modulate the anchoring of H₂-VGGVG-OH (unprotected) and Boc-VGGVG-OEt (terminal protected) peptides, respectively.

Based on these premises, Figures 6 and 7, selected among the relevant supplementary figures, are reported to represent the best Pt/PoAP/ELP combination of each monomer for sensing amyloid fibrils.

Figures 6 compare XPS C1s spectra and AFM images of the Pt/PoAP/ELP electrode (resulting from Pt/PoAP exposition to 'unprotected' VGGVG solutions aged for 15 days), before (6a,b) and after (6c,d) detection of (VGGVG)₃. Similarly, Figures 7 compare XPS C1s spectra and AFM images of

Pt/PoAP/ELP electrodes (resulting from Pt/PoAP exposition to 'protected' VGGVG 'fresh' solutions), before (7a,b) and after (7c,d) detection of (VGGVG)₃.

Both figures testify a considerable attachment of the trimer fibrils on the surface of both selected Pt/PoAP/ELP systems, both having oxygenated functionalities properly exposed outward, as explained in supplementary materials and in points a, b of the above summary.

To verify if unwanted precipitation could be contributing to the attachments of ELP monomers on Pt/PoAP surfaces and be misinterpreted for specific adsorption, experiments with the 'protected' monomer at different ageing time were repeated using platinum foil as interacting surface. AFM images indicate no specific interactions between Pt and ELPs (Figure S6).

However, as for the experiments with fresh PoAP in Figures 3 and for the fresh VGGVG in S1, it would be expected a very tiny ELP adsorption also on platinum, not detectable by AFM. In fact, as revealed by surface mass spectrometry [38], the growth of PoAP chains, at the platinum sites during CV electro-synthesis, was reported to begin with the nitrogen atom of the oxidized monomer, oAP. Thus, a likely interaction with nitrogen, ELP-specific element, could be only indicative of Pt/PoAP synergy and of the benefit of using platinum substrate for ELP detection, vide infra.

Given these outcomes, in order to complete our study, in view of preventing also the possible occurrence of local detachments favored by the subsequent adsorbing steps of the procedure and make the stratified assembly easier to be prepared, more reproducible and possibly more efficient, the adsorption of ELP monomer on PoAP surface, as method of immobilization, was changed to entrapping at or near PoAP surface, during CV electrosynthesis.

It is worth noting that the template electro-polymerization of poly o-aminophenol was successfully attempted with specific proteins [55], therefore, we sought to adapt to our purposes the same procedure, normally adopted for the *surface imprinting*. Thus, ELP monomers, either terminal protected and unprotected, were added during CV electro-synthesis of the ultrathin PoAP membrane to be therein entrapped as surface receptors, as detailed in the next paragraph. The whole system was tested by XPS and AFM, before and after immersion in the aged suspension of trimer fibrils, also considering the influence of the underneath platinum.

d) Study of PoAP and (VGGVG)₃ interactions, mediated by VGGVG monomers entrapped on PoAP surfaces during CV electro-synthesis: influence of VGGVG terminal groups

As anticipated, this procedure recalls the bi-dimensional MIP methodology [43,46,55] here revised to entrap, irreversibly, each monomer without its removal at the end of the electro-synthesis. The expectation was to have the monomer(s) firmly anchored at (or near at) the polymer surface, with the functional groups of either side not fully engaged in reciprocal bonds and thus available to intercept longer ELP sequences, as those of the trimer' type.

Figures 8 show the CV electro-synthesis performed as usual, with the same number of scans, 1 to 20 cycles, used for insulating PoAP [25-27] with addition of unprotected (a) and protected (b) VGGVG at the end of the first scan.

In comparison to the CV growth of insulating PoAP [26], the CVs reported in Figure 8a,b show a current re-increase after the addition of monomer(s) over the almost complete attenuation normally recorded after the first cycle. The increase, of lower entity, for the protected monomer, may signify 're-exposure' of platinum sites, electro-active for oAP polymerization, due to 'displacement and /or re-alignment' of polymer chains deposited during the first cycle.

The AFM images of Figure 9a, very similar to those of insulating PoAP, suggest that unprotected monomer is smoothly incorporated within the polymer chains without altering the PoAP morphology. In parallel, carbon spectra show additional contribution for the monomer presence, but with no appreciable changes of the overall carbon shape as well as of the Pt/N ratio, indicative of substrate coverage. The surface offered to fibrils by the layered Pt/PoAP/ELP-unprotected shows an increment of interacting groups, carbonyl- and carboxyl-like with respect to the 'inactive' Pt/PoAP freshly prepared.

On the other side, AFM images and XPS spectra of Figure 9b indicate a less compact and homogeneous deposit when the protected monomer is added during PoAP electro-synthesis and evident changes of the carbon and platinum peak shapes, respectively. In particular, Figure 9b shows a different relative intensity of the carbon peaks compared to Figure 9a with abatement of aliphatic components and further increment of carbonyl/carboxyl groups and a double chemical state for platinum. Going more in detail, the curve-fitting results, shown in Table 2, indicate the main carbon components of Figures 9a,b, fitted with the same peak parameters, to have similar chemical state assignments, eventually including closely-spaced chemical states, but remarkably different in their relative intensity. Moreover, the usual 4f doublet of metallic platinum [27] is shown to be split in figure 9b, the component at the higher BE, unexpectedly, lying in the energy interval characteristic of oxidized platinum. Taken together with the less marked increase of the

anodic current of Figure 8b, these results may imply a direct interaction of the protected monomer with the platinum substrate causing a partial steric hindrance towards oAP oxidation, most likely, by means of the aliphatic protecting groups.

A possible explanation from these preliminary results could be given considering the monomer(s) influence on PoAP deposition, within the second and the twentieth cycle, as clearly perceived from the CVs comparison of Figures 8. In fact, as known from previous studies, at the end of the first cycle the platinum sites are almost, but not fully saturated yet, whereas oAP oxidation, followed by attachment of short PoAP chains in vertical alignment to best accommodate vicinal chains, is found to be completed at around the twentieth cycle, when the current is fully attenuated [25-27]. Thus, ELP monomer(s) added at the end of the first cycle, upon its entrapping inside PoAP, could interfere by displacing the deposited chains, by fastening their alignment and, eventually, by interacting with the electro-active platinum sites, uncovered by this induced displacement/alignment of PoAP chains.

As for the adsorption method, the whole matter can be better reasoned by defining the interacting surfaces seen by the fibrils, therefore, the performance of the two systems in the presence of (VGGVG)₃ fibrils was investigated.

Figures 10 compare XPS C1s regions and AFM images of the two Pt/PoAP/ELP systems made of unprotected (10a) and protected (10b) VGGVG monomers, after interaction with the trimer (VGGVG)₃ in form of fibrillar aggregates. Remarkably, Figures 10a,b undoubtedly prove the ability of both systems to detect fibrillar aggregates. (VGGVG)₃ fibrils are easily recognizable in AFM images and from XPS analysis, with both C1s profiles recalling that of the trimer, given the massive fibrils adsorption. As for Figures 9, the carbon spectra of Figures 10 were resolved into components by curve-fitting. Results confirm the significant presence of ELP components for both cases, although a greater interactions was observed for the system made of protected monomer.

Although further investigation are required to fully understand the mechanisms governing these Pt/PoAP/ELP interactions, nevertheless layered systems based on monomers entrapments prove to be the most promising as bio-detectors, performing with high specificity towards amyloid fibrils.

The greater degree of fibrils interaction with the system made of protected monomer can be explained by its wider bio-receptors distribution along the exposing surface due to different 'entrapping' sites of the monomer itself, including platinum substrate, acting in synergy. It is equally important to preserve the intact coverage of the electrode substrate, better ensured by the

unprotected monomer, for avoiding its poisoning. Moreover, for a good fibrils detection, a too massive absorption is not so recommended if we consider that a possible detachment could take place subsequently, perhaps even during ongoing measurements.

CONCLUSIONS

All together results from the present study provide unequivocally evidence of the forces that are driving the mutual interaction of the investigated biomolecules.

The insulating PoAP, electro-synthesized on platinum has proven useful to efficiently adsorb/entrap ELP monomers on its surface and can be used as receptors of ELP fibrils, relying on interacting forces, similar to those inducing ELPs self-assembly, favored by the anchoring of the monomer sequences.

The best Pt/PoAP/ELP assembly to detect ELP fibrils, (VGGVG)₃, requires the outer surface exposing the right number and disposition of 'anchoring' carbonyls, as also demonstrated by the augmented efficacy of Pt/PoAP electrode, alone, when stored in air for days, due to the increment of carbonyls by post-synthesis oxidation of -C=N< groups.

In the perspective of proposing an optimal performing biosensor for amyloid detection, various combinations of Pt/PoAP/ELP assembly were investigated, evaluating the influence of the following variables:

- aging time of the VGGVG monomers solution influences aggregation mechanisms of (VGGVG)_n sequences, even for the shortest ones (n=1), thus providing new information on the kinetics of aggregation and on the mechanism of fibrils' nucleation
- presence of protective terminal groups induces a different kind of interaction with the PoAP substrate: hydrophobic forces were prominent for Boc-VGGVG-OEt, whereas H-bonds between carbonyls were prevalent for H₂-VGGVG-OH
- two methods of immobilization of ELP monomers, namely the adsorption method and the surface imprinting method based on bi-dimensional MIP, were compared by exposing Pt/PoAP/ELP electrodes to VGGVG trimer in order to evaluate their efficacy in recognizing amyloid fibrils in solution .

Results show the advantage of the modified bi-dimensional MIP methodology, fast to prepare and to reproduce, to efficiently retain on Pt/PoAP surface the imprinted ELP monomer(s) as bio-detectors. Indeed, their ability to detect fibrillar aggregates was amply proved, in this work.

We therefore believe that, if properly conveyed, these MIP-based systems have the right characteristics to be the receptor components of a biosensor device for neurodegenerative diseases, as Alzheimer Disease.

ACKNOWLEDGMENTS

The authors are grateful to Dr. Fausto Langerame for XPS acquisitions and technical assistance.

The availability of the 'Surface Microscopy' Laboratory of the Science Department (University of Basilicata) are acknowledged for the use of electrochemical and AFM instrumentation, respectively, during the PhD thesis of M.E.E Carbone (A.Y. 2015-2016).

CONFLICT OF INTEREST

The authors declare that there are no known conflicts of interest regarding the publication of this article.

REFERENCES

- [1] Takahashi RH, Nagao T, Gouras GK. Plaque formation and the intraneuronal accumulation of β -amyloid in Alzheimer's disease. *Pathol Int.* 2017; 67:185-93.
- [2] Hung ASM, Liang Y, Chow TC, Tang HC, Wu SL, Wai MSM, Yew DT. Mutated tau, amyloid and neuroinflammation in Alzheimer disease—A brief review. *Prog Histochem Cytochem.* 2016; 51:1-8.
- [3] Selkoe DJ and Hardy J. The amyloid hypothesis of Alzheimer's disease at 25 years. *EMBO Mol. Med.* 2016; 8:595-608.
- [4] Kaushik A, Jayant RD, Tiwari S, Vashist A, Nair M. Nano-biosensors to detect beta-amyloid for Alzheimer's disease management. *Biosens Bioelectron.* 2016; 80:273-87.
- [5] Shui B, Tao D, Florea A, Cheng J, Zhao Q, Gu Y, Li W, Jaffrezic-Renault N, Mei Y, Guo Z. Biosensors for Alzheimer's disease biomarker detection: A review, *Biochimie* 2018, 147:13-24
- [6] Xing Y and Xia N. Biosensors for the Determination of Amyloid-Beta Peptides and their Aggregates with Applicatin to Alzheimer's Disease. *Analytical Letters* 2015, 48: 879–893.
- [7] Poljak A and Sachdev PS. Plasma amyloid beta peptides: an Alzheimer's conundrum or a more accessible Alzheimer's biomarker? *Expert Rev Neurother,* 2017, 17: 3–5.
- [8] Moulin S, Leys D, Schraen-Maschke S, et al. Abeta1-40 and Abeta1-42 plasmatic levels in stroke: influence of pre-existing cognitive status and stroke characteristics. *Curr Alzheimer Res.* 2015, 12:1–9.
- [9] Ganesh HV, Chow AM, Kerman K. Recent advances in biosensors for neurodegenerative disease detection. *TrAC-Trend Anal Chem.* 2016; 79:363-70.
- [10] Bochicchio B, Lorusso M, Pepe A, Tamburro AM. On enhancers and inhibitors of elastin-derived amyloidogenesis. *Nanomedicine* 2009; 4:31-46.
- [11] Zhao J, Gao T, Yan Y, Chen G, Li G. Probing into the interaction of β -amyloid peptides with bilayer lipid membrane by electrochemical techniques. *Electrochem Commun.* 2013; 30:26-8.
- [12] Okuno H, Mori K, Okada T, Yokoyama Y, Suzuki H. Development of aggregation inhibitors for amyloid- β peptides and their evaluation by quartz-crystal microbalance. *Chem Biol Drug Des.* 2007; 69:356-61.
- [13] Okuno H, Mori K, Jitsukawa T, Inoue H, Chiba S. Convenient Method for Monitoring A β Aggregation by Quartz-Crystal Microbalance. *Chem Biol Drug Des.* 2006; 68:273-75.
- [14] Knowles TP, Shu W, Devlin GL, Meehan S, Auer S, Dobson CM, Welland ME. Kinetics and thermodynamics of amyloid formation from direct measurements of fluctuations in fibril mass. *Proc Natl Acad Sci U S A.* 2007; 104:10016–21.

- [15] White DA, Buell AK, Dobson CM, Welland ME, Knowles TP. Biosensor-based label-free assays of amyloid growth. *FEBS Lett.* 2009; 583:2587-92.
- [16] Mustafa MK, Nabok A, Parkinson D, Tothill IE, Salam F, Tsargorodskaya A. Detection of β -amyloid peptide (1–16) and amyloid precursor protein (APP 770) using spectroscopic ellipsometry and QCM techniques: A step forward towards Alzheimers disease diagnostics. *Biosens Bioelectron.* 2010; 26:1332-6.
- [17] Gagni P, Sola L, Cretich M, Chiari M. Development of a high-sensitivity immunoassay for amyloid-beta 1–42 using a silicon microarray platform. *Biosens Bioelectron* 2013, 47:490-5.
- [18] Stravalaci M, Bastone A, Beeg M, Cagnotto A, Colombo L, Di Fede G, Tagliavini F, Cantù L, Del Favero E, Mazzanti M, Chiesa R, Salmona M, Diomedea L, Gobbi M. Specific recognition of biologically active amyloid- β oligomers by a new surface plasmon resonance-based immunoassay and an in vivo assay in *Caenorhabditis elegans*. *J Biol Chem.* 2012; 287:27796-805.
- [19] Choi I, Lee LP. Rapid detection of A β aggregation and inhibition by dual functions of gold nanoplasmonic particles: Catalytic activator and optical reporter. *ACS Nano.* 2013; 7:6268-77.
- [20] Ragaliauskas T, Mickevicius M, Budvytyte R, Niaura G, Carbonnier B, Valincius G. Adsorption of β -amyloid oligomers on octadecanethiol monolayers. *J Colloid Interf Sci.* 2014; 425:159-167.
- [21] Becherer T, Grunewald C, Engelschalt V, Multhaupt G, Risse T, Haag R. Polyglycerol based coatings to reduce non-specific protein adsorption in sample vials and on SPR sensors. *Anal Chim Acta.* 2015; 867:47-55.
- [22] Buell AK, White DA, Meier C, Welland ME, Knowles TP, Dobson CM. Surface attachment of protein fibrils via covalent modification strategies. *J Phys Chem B.* 2010; 114:10925–38.
- [23] Kotarek JA, Johnson KC, Moss MA. Quartz crystal microbalance analysis of growth kinetics for aggregation intermediates of the amyloid- β protein. *Anal Biochem.* 2008;378:15-24
- [24] Valiaev A, Abu-Lail NI, Lim DW, Chilkoti A, Zauscher S. Microcantilever sensing and actuation with end-grafted stimulus-responsive elastin-like polypeptides. *Langmuir*, 2007; 23:339-44.
- [25] Carbone ME, Ciriello R, Guerrieri G, Langerame F, Salvi AM. XPS, AFM and electrochemical investigation on the inner composition of insulating poly(o-aminophenol), PoAP, deposited on platinum by CV, as a function of the number of cycles, *Surf Interface Anal.* 2016; 48:99-104.
- [26] Carbone ME, Ciriello R, Guerrieri G, Salvi AM. XPS investigation on the chemical structure of a very thin, insulating, film synthesized on platinum by electropolymerization of o-aminophenol (oAP) in aqueous solution at neutral pH, *Surf Interface Anal.* 2014; 46:1081-5.

- [27] Carbone ME, Ciriello R, Guerrieri G, Salvi AM. Poly (o-aminophenol) Electrosynthesized onto Platinum at Acidic and Neutral pH: Comparative Investigation on the Polymers Characteristics and on Their Inner and Outer Interfaces. *Int. J. Electrochem. Sci.* 2014;9:2047-66.
- [28] Carbone ME, Ciriello R, Granafei S, Guerrieri G, Salvi AM. Electrosynthesis of conducting poly (o-aminophenol) films on Pt substrates: a combined electrochemical and XPS investigation. *Electrochim Acta* 2014; 144:174-85.
- [29] Carbone ME, Ciriello R, Granafei S, Guerrieri G, Salvi AM. EQCM and XPS investigations on the redox switching of conducting poly (o-aminophenol) films electrosynthesized onto Pt substrates. *Electrochim Acta* 2015; 176: 926-40.
- [30] Salvi AM, Moscarelli P, Bochicchio B, Lanza G, Castle JE. Combined effects of solvation and aggregation propensity on the final supramolecular structures adopted by hydrophobic, glycine-rich, elastin-like polypeptides. *Biopolymers* 2013; 99:292-313.
- [31] Salvi AM, Moscarelli P, Satriano G, Bochicchio B, Castle JE. Influence of amino acid specificities on the molecular and supramolecular organization of glycine-rich elastin-like polypeptides in water. *Biopolymers*, 2011; 95:702-21.
- [32] Castle JE, Ibris N, Salvi AM, Moscarelli P, Bochicchio B, Pepe A. Characterisation of helical structure in AFM micrographs of a trimer of the peptide sequence (ValGlyGlyValGly). *Surf Interface Anal.* 2014; 46:679–682.
- [33] Flamia R, Salvi AM, D'Alessio L, Castle JE, Tamburro AM. Transformation of amyloid-like fibers, formed from an elastin-based biopolymer, into a hydrogel: an X-ray photoelectron spectroscopy and atomic force microscopy study. *Biomacromolecules*, 2007; 8:128-38.
- [34] Flamia R, Lanza G, Salvi AM, Castle JE, Tamburro AM. Conformational study and hydrogen bonds detection on elastin-related polypeptides using X-ray photoelectron spectroscopy. *Biomacromolecules*, 2005; 6:1299-309.
- [35] Moscarelli P, Boraldi F, Bochicchio B, Pepe A, Salvi AM, Quaglino D. Structural characterization and biological properties of the amyloidogenic elastin-like peptide (VGGVG)₃. *Matrix Biol.* 2014; 36:15-27.
- [36] Boraldi F, Moscarelli P, Bochicchio B, Pepe A, Salvi AM, Quaglino D. Heparan sulfate facilitate harmless amyloidogenic fibril formation interacting with elastin-like peptides. *Sci. Rep.* 2018; 8: 3115.
- [37] Carbone ME, Castle JE, Ciriello R, Salvi AM, Treacy J, Zhdan P, In Situ Electrochemical–AFM and Cluster-Ion-Profiled XPS Characterization of an Insulating Polymeric Membrane as a Substrate for Immobilizing Biomolecules, *Langmuir* 2017; 33:2504-13.
- [38] Carbone ME, Ciriello R, Salvi AM, Castle JE. ToF-SIMS study of stages in the electrochemical growth of insulating Poly(o-aminophenol) films, *Surf Interface Anal.* 2016; 48:644-48.

- [39] Fandrich M. On the structural definition of amyloid fibrils and other polypeptide aggregates. *Cell. Mol. Life Sci.* 2007, 64: 2066-78.
- [40] Ruggeri FS, Habchi J, Cerreta A, Dietler G. AFM-Based Single Molecule Techniques: Unraveling the Amyloid Pathogenic Species. *Current Pharmaceutical Design* 2016, 22: 3950-3970
- [41] Wei G, Su Z, Reynolds NP, Arosio P, Hamley IW, Gazit E, Mezzenga R. Self-assembling peptide and protein amyloids: from structure to tailored function in nanotechnology. *Chem. Soc. Rev.* 2107, 46: 4661-4708.
- [42] Zhang W, Yu X, Li Y, Su Z, Jandt KD, Wei G. Protein-mimetic nanofibers: Motif design, self-assembly synthesis, and sequence-specific biomedical applications. *Progress in Polymer Science.* Article In Press. Available online 16 December 2017
- [43] Yin D, Ulbricht M, Protein-selective adsorbers by molecular imprinting via a novel two-step surface grafting method. *J. Mater. Chem B*, 2013, 1: 3209-3219.
- [44] Saridakis E, Chayen NE, Imprinted polymers assisting protein crystallization. *Trends Biotechnol* 2013, 31: 515-520.
- [45] Malitesta C, Mazzotta E, Picca RA, Poma A, Chianella I, Piletsky SA. MIP sensors--the electrochemical approach. *Anal Bioanal Chem* 2012, 402: 1827-1846.
- [46] Turner NW, Jeans CW, Brain KR, Allender CJ, Hlady V, Britt DW. From 3D to 2D: A Review of the Molecular Imprinting of Proteins *Biotechnol. Progr.* 2006, 22(6): 1474-1489
- [47] Ortega JM. Conducting potential range for poly (o-aminophenol). *Thin Solid Films*, 2000; 371: 28-3.
- [48] Flamia R, Zhdan PA, Martino M, Castle JE, Tamburro AM. AFM study of the elastin-like biopolymer poly (ValGlyGlyValGly). *Biomacromolecules*, 2004; 5:1511-1518.
- [49] Castle JE, Chapman-Kpodo , Proctor A., Salvi AM. Curve-fitting in XPS using extrinsic and intrinsic background structure. *Journal of Electron Spectroscopy and Related Phenomena* 2000, 106: 65-80.
- [50] Castle JE, Salvi AM. Chemical state information from the near-peak region of the X-ray photoelectron background. *J Electron Spectrosc.* 2001; 114:1103-13.
- [51] NIST database. <http://www.nist.gov/srd/surface.htm> (last accessed 2017).
- [52] Seah MP, Briggs D, Grant JT, Surface analysis by auger and X-ray photoelectron spectroscopy. Chichester: IM Publications and Surface Spectra; 2003.
- [53] Wagner CD, Davis LE, Zeller MV, Taylor JA, Raymond RH, Gale LH. Empirical atomic sensitivity factors for quantitative analysis by electron spectroscopy for chemical analysis. *Surf Interface Anal.* 1981; 3:211-25.

1
2
3
4
5
6
7
8
9
10
11
12
13
14
15
16
17
18
19
20
21
22
23
24
25
26
27
28
29
30
31
32
33
34
35
36
37
38
39
40
41
42
43
44
45
46
47
48
49
50
51
52
53
54
55
56
57
58
59
60

[54] Castiglione Morelli MA, DeBiasi M, DeStradis A, Tamburro AM. An aggregating elastin-like pentapeptide. *J Biomol Struct Dyn* 1993; 11:181-90.

[55] Felismina T.C. Moreira , Sanjiv Sharma, Rosa A.F. Dutrae, João P.C. Noronha, Anthony E.G. Cass, M. Goreti F. Sales. Protein-responsive polymers for point-of-care detection of cardiac biomarker. *Sensors and Actuators B* 2014, 196: 123–132

For Peer Review

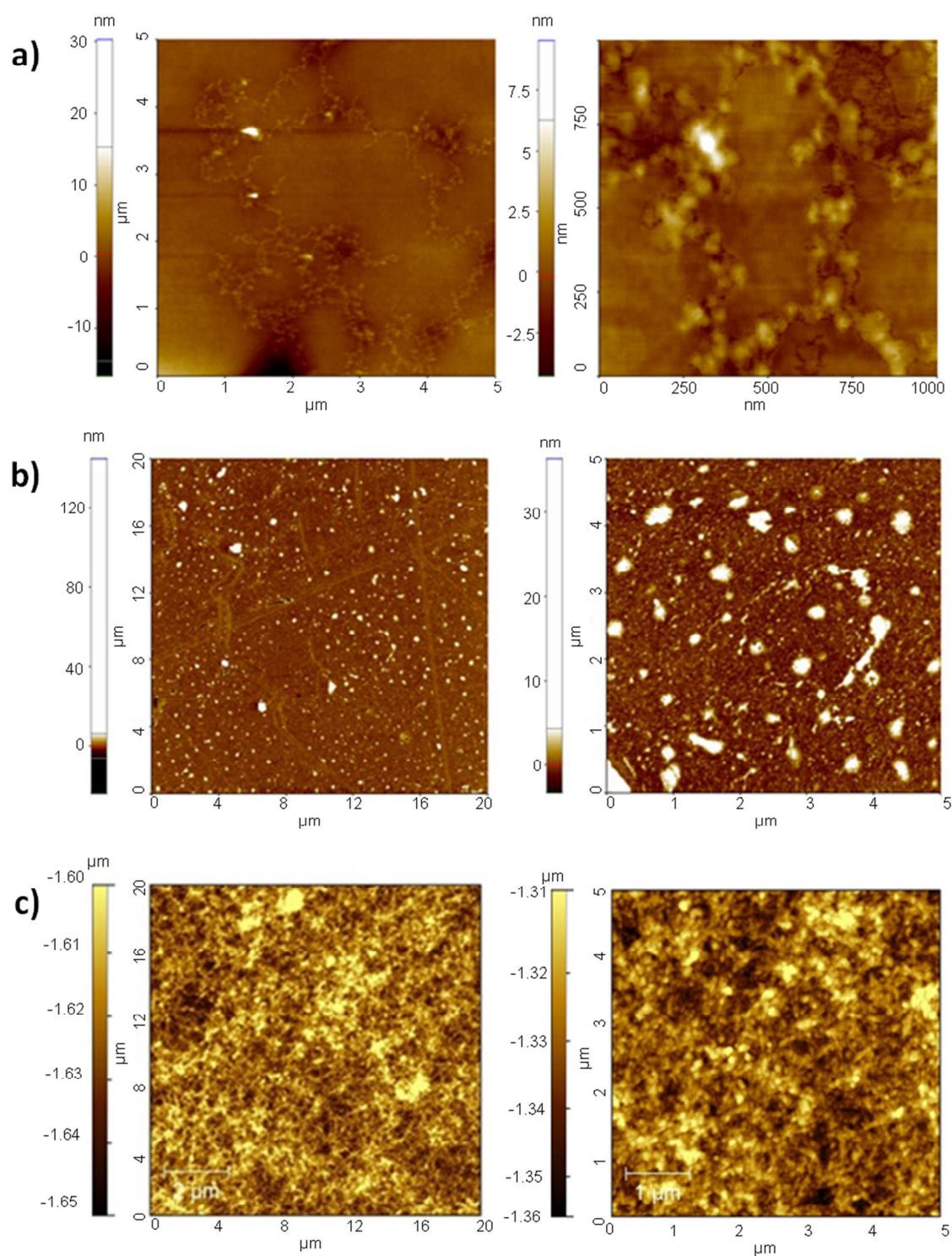


Fig.1 AFM images of VGGVG (a) BocVGGVGOEt (b) and (VGGVG)₃ (c) water suspension (0.1 mg/mL) deposited on silicon wafer.

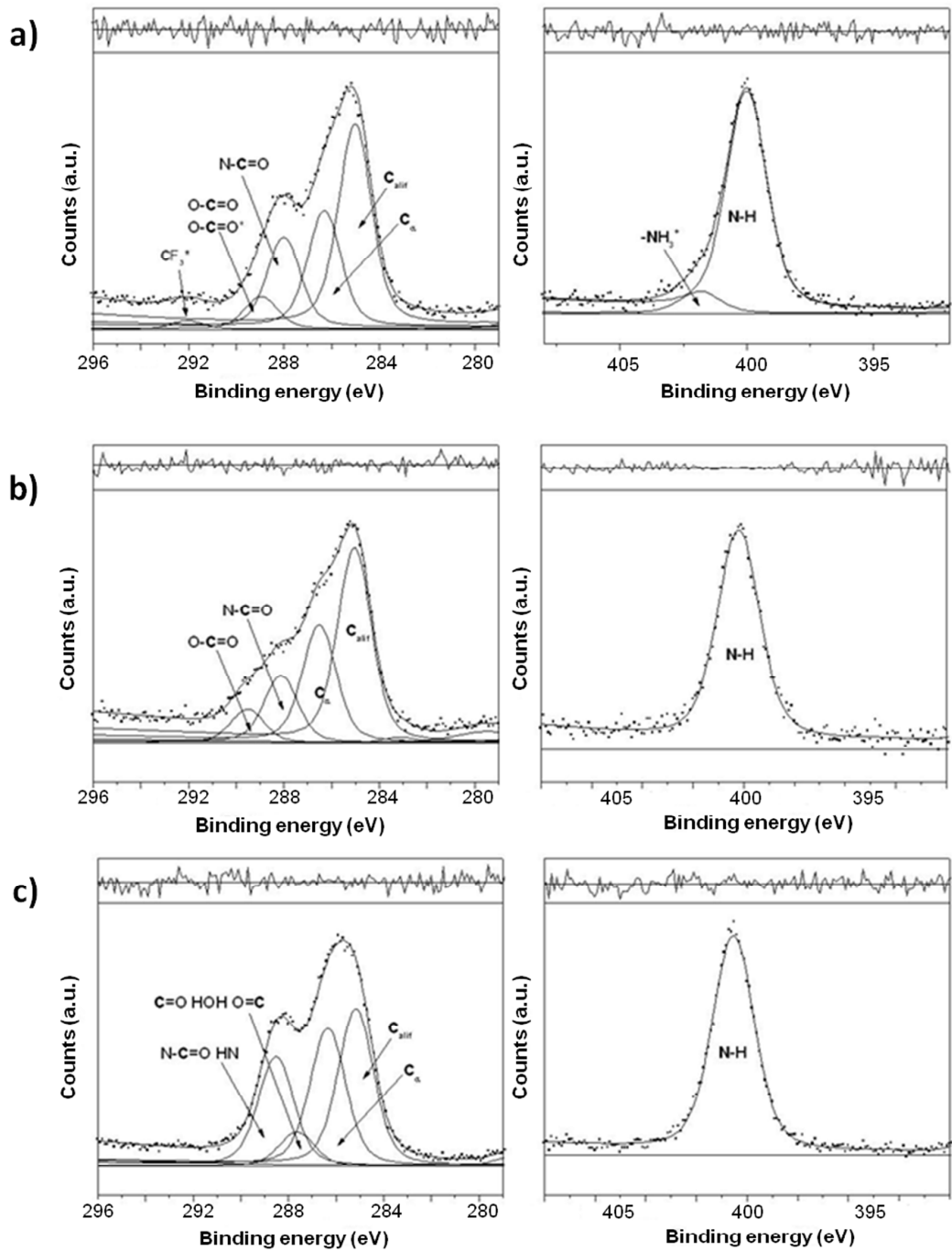


Fig.2 XPS curve-fitted C1s and N1s spectra of VGGVG (a) BocVGGVGOEt (b) and (VGGVG)₃ (c) water suspension (0.1 mg/mL) deposited on silicon wafer. Curve-fitting results are reported in Table 1 The O1s regions of monomer deposits (2a,2b) are not reported due to the substrate signals interference. Results of the curve-fitted O1s region of the trimer deposits(2c) are reported in Table 1

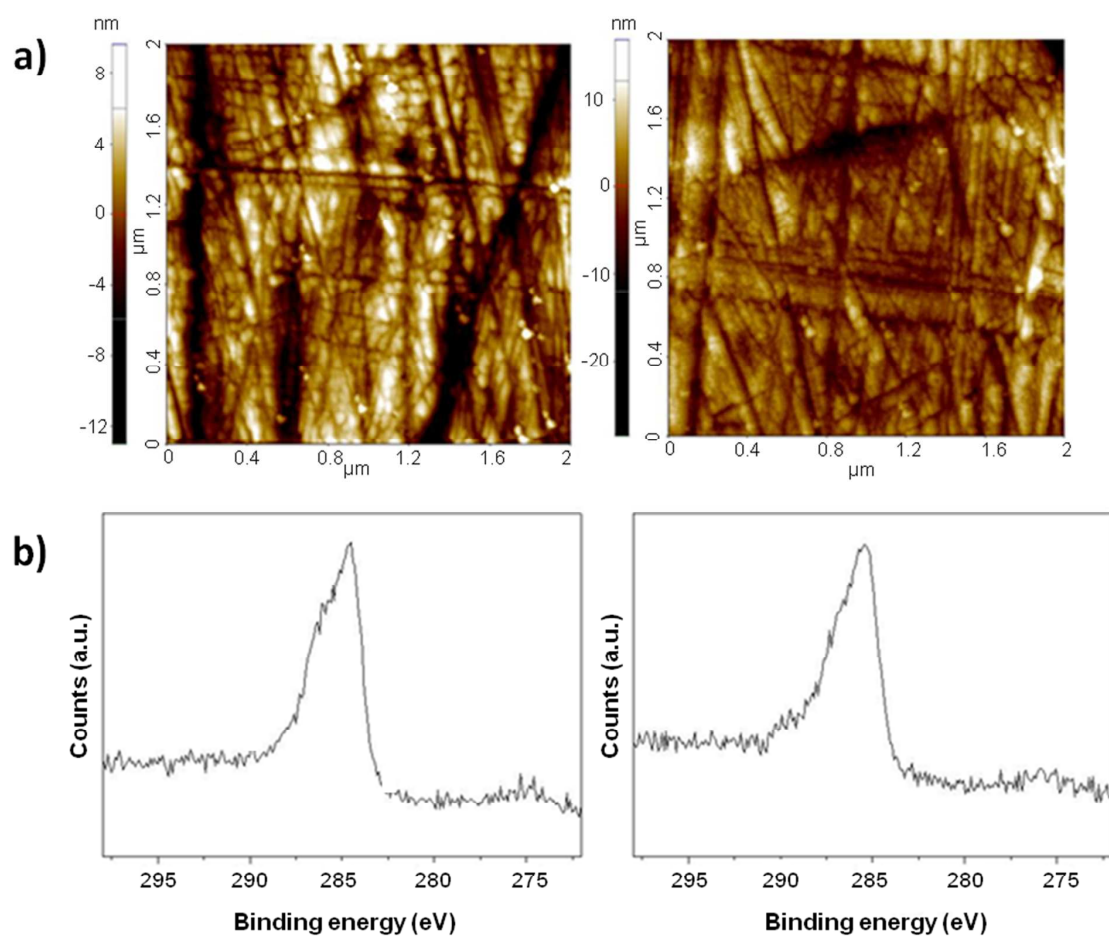


Fig.3 Interaction of insulating PoAP with (VGGVG)₃ solution: AFM images and XPS C1s spectra of the PoAP before (on the left) and after (on the right) exposure to (VGGVG)₃ solution.

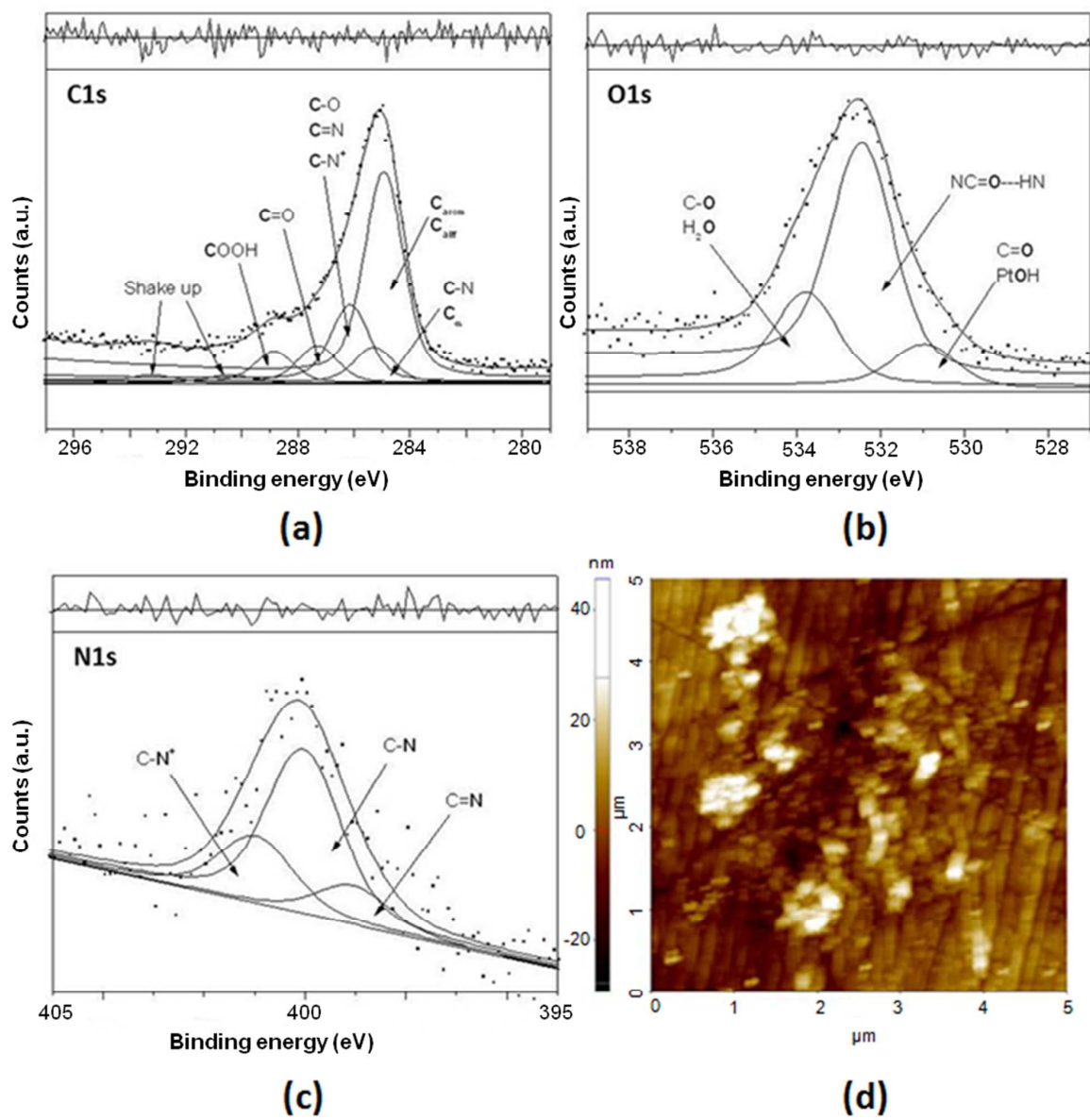


Fig.4 XPS curve-fitted C1s (a), O1s (b), N1s regions (c) and AFM images 5x5 μm, (d) of insulating PoAP aged 15 days and then exposed for 6 h at 37 °C to the solution of (VGGVG)₃. Curve-fitting results are reported in Table 2.

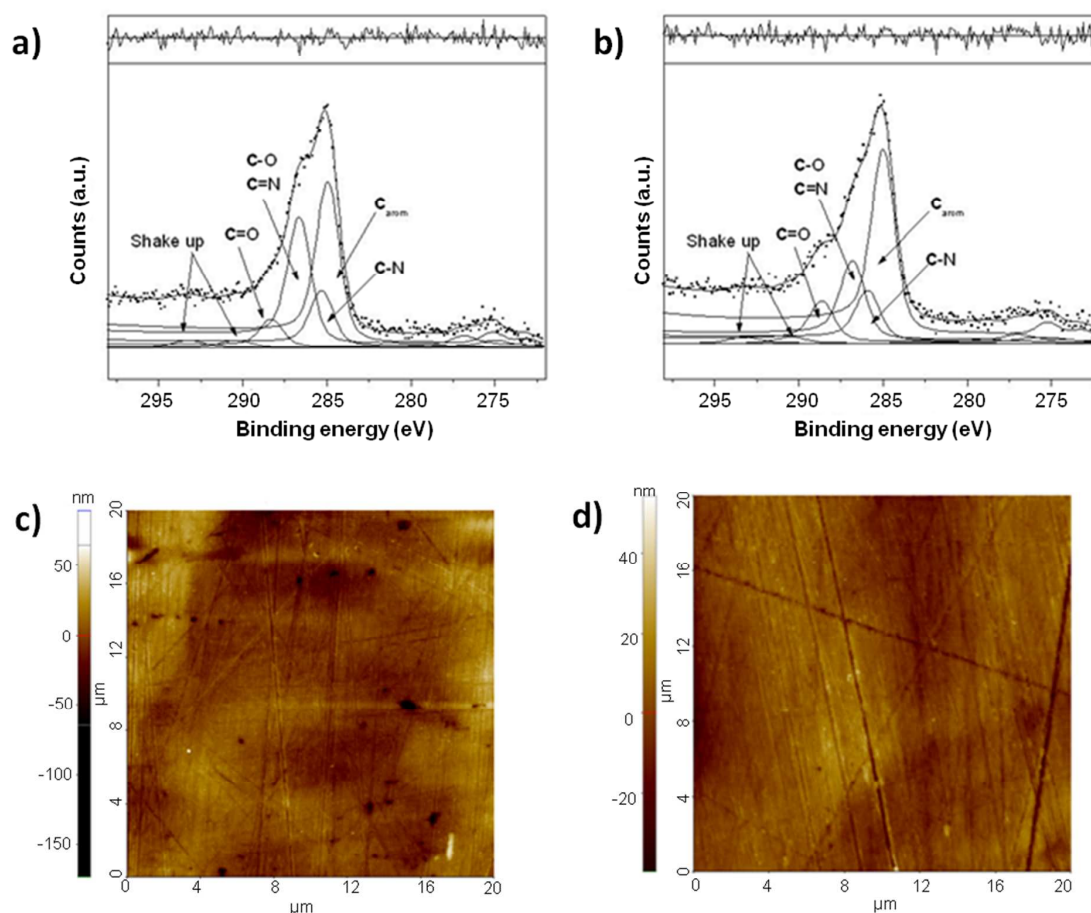


Fig.5 XPS curve-fitted C1s region of the insulating PoAP analyzed immediately after the electrosynthesis (a) and after 15 days of aging in air at room temperature (b) and relevant AFM images (c,d). Curve-fitting results are reported in Table 2.

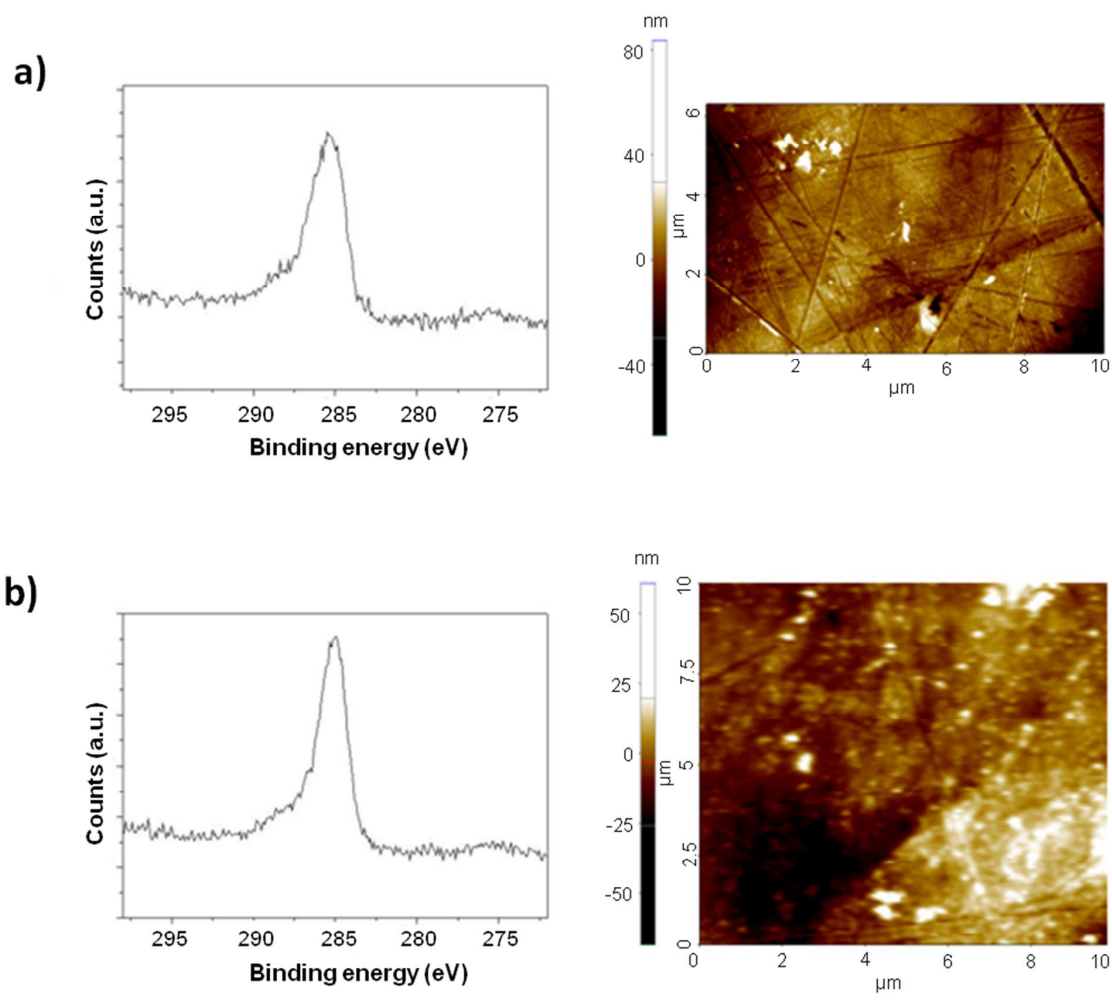


Fig.6 XPS C1s spectra and AFM images of the Pt/PoAP electrodes exposed to 15 days aged VGGVG solutions (on the left); XPS C1s spectra and AFM images of the detection of (VGGVG)₃ (on the right).

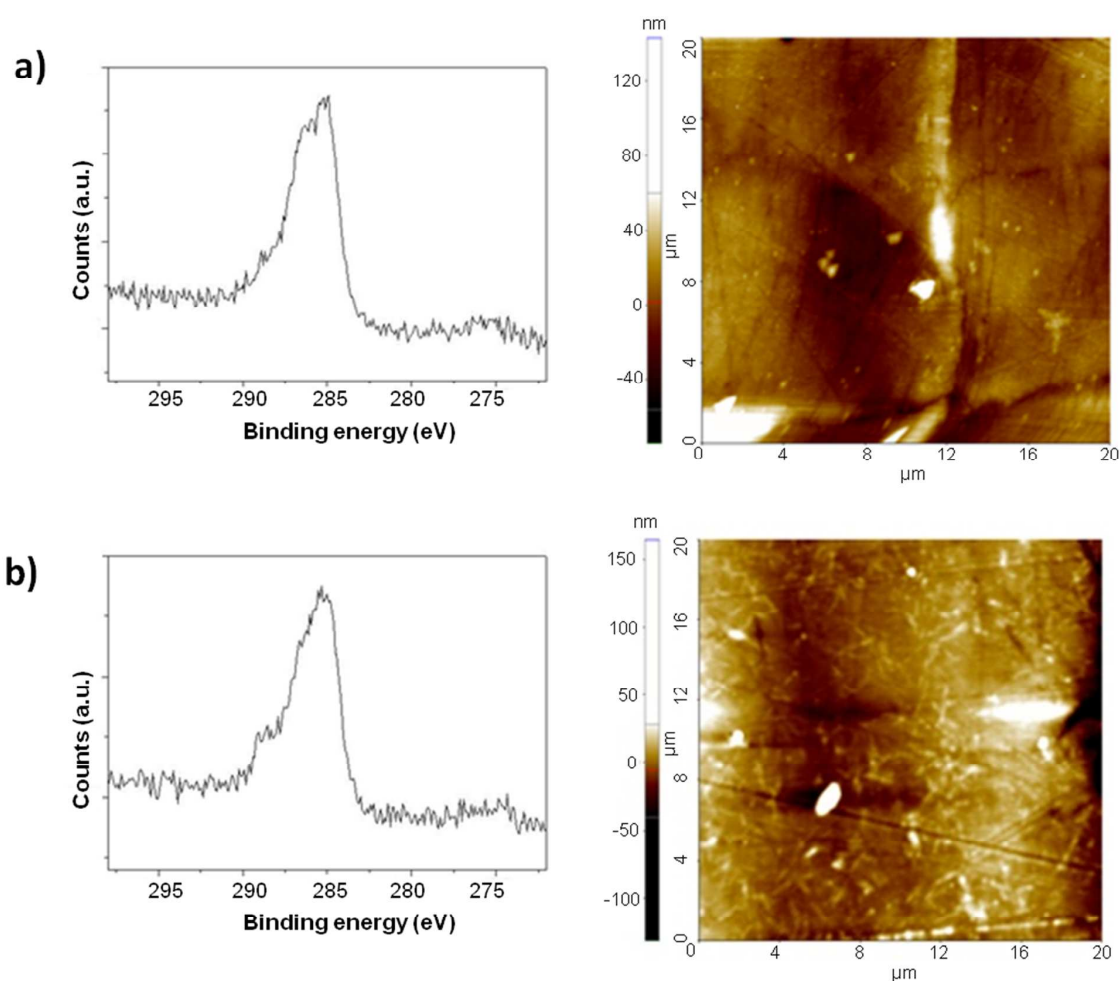


Fig.7 Interaction of insulating PoAP with BocVGGVGOEt solutions: XPS C1s spectra and AFM images of the Pt/PoAP electrodes exposed to fresh protected-VGGVG solutions (on the left); XPS C1s spectra (on the left) and AFM images (on the right) of the detection of (VGGVG)₃ (on the right).

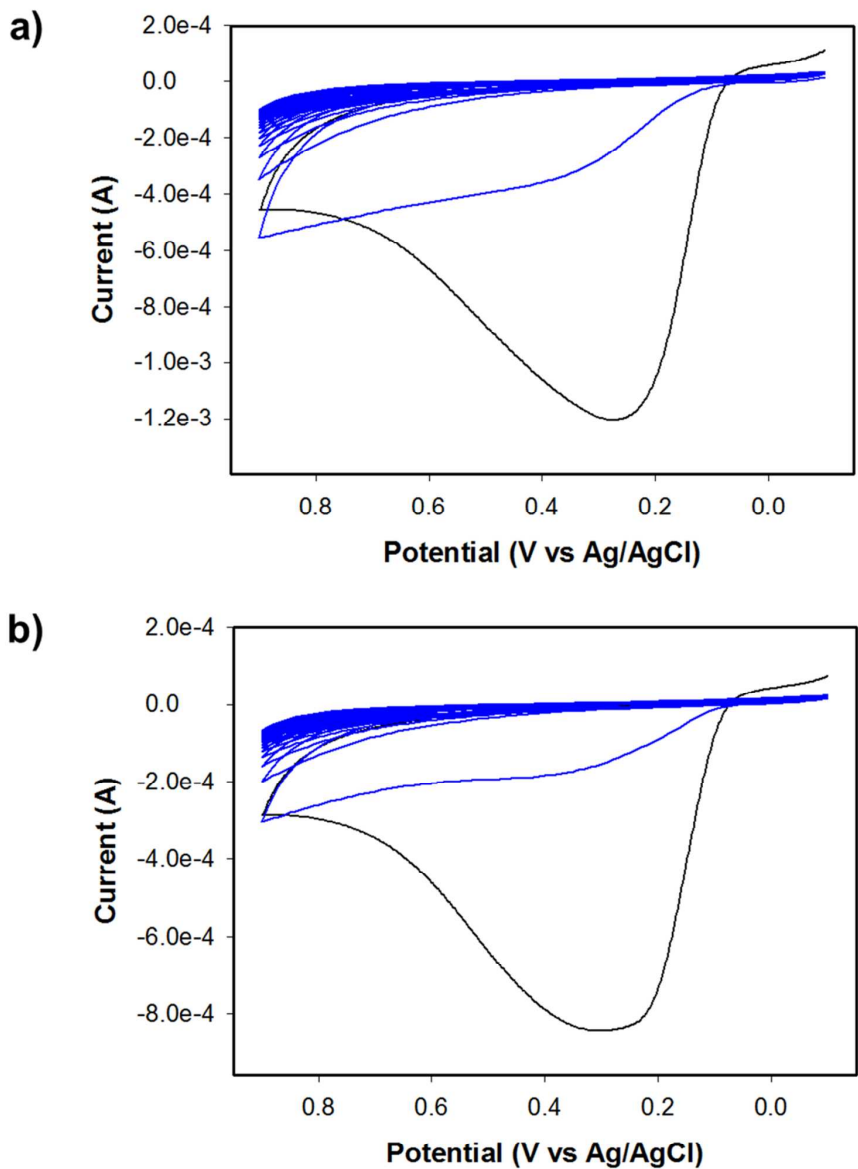


Fig.8 Cyclic voltammetry of electrosynthesis of insulating PoAP on platinum electrode with a scan rate of 50 mV/s: the first voltammetric cycle (in Black) is registered in 5 mM oAP solution in phosphate buffer (I = 0.1M, pH = 7.0), while the other nineteenth scan are acquired after the addition of an aqueous solution of VGGVG (A) and BocVGGVGOEt (B) at a concentration of 0.1 mg/mL.

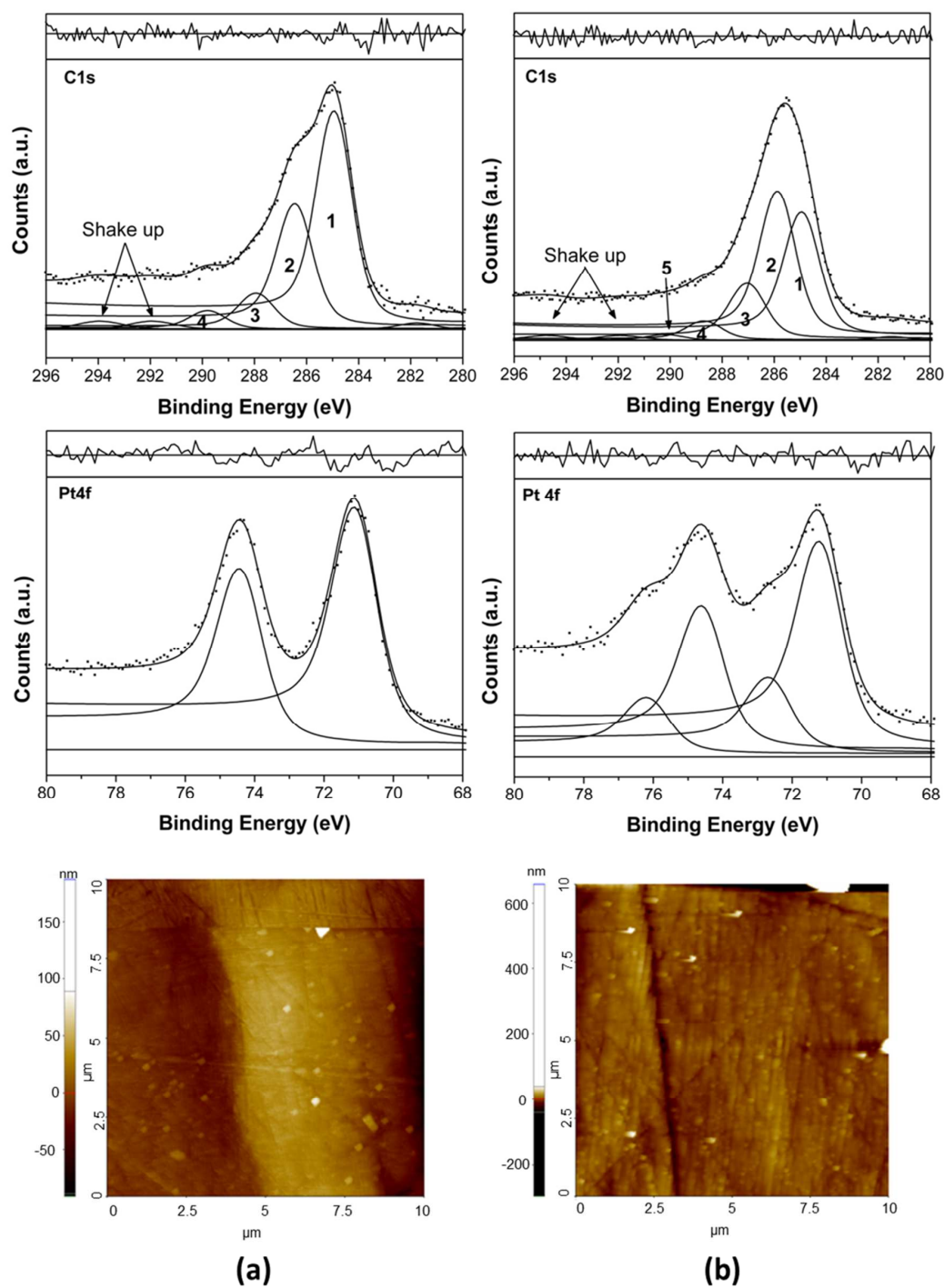


Fig.9 XPS curve fitted C1s and Pt4f regions of PoAP with entrapped VGGVG (A) and BoCVGGVGOEt (B) and relevant AFM images at 10x10 μm magnification. Curve-fitting results are reported in Table 2.

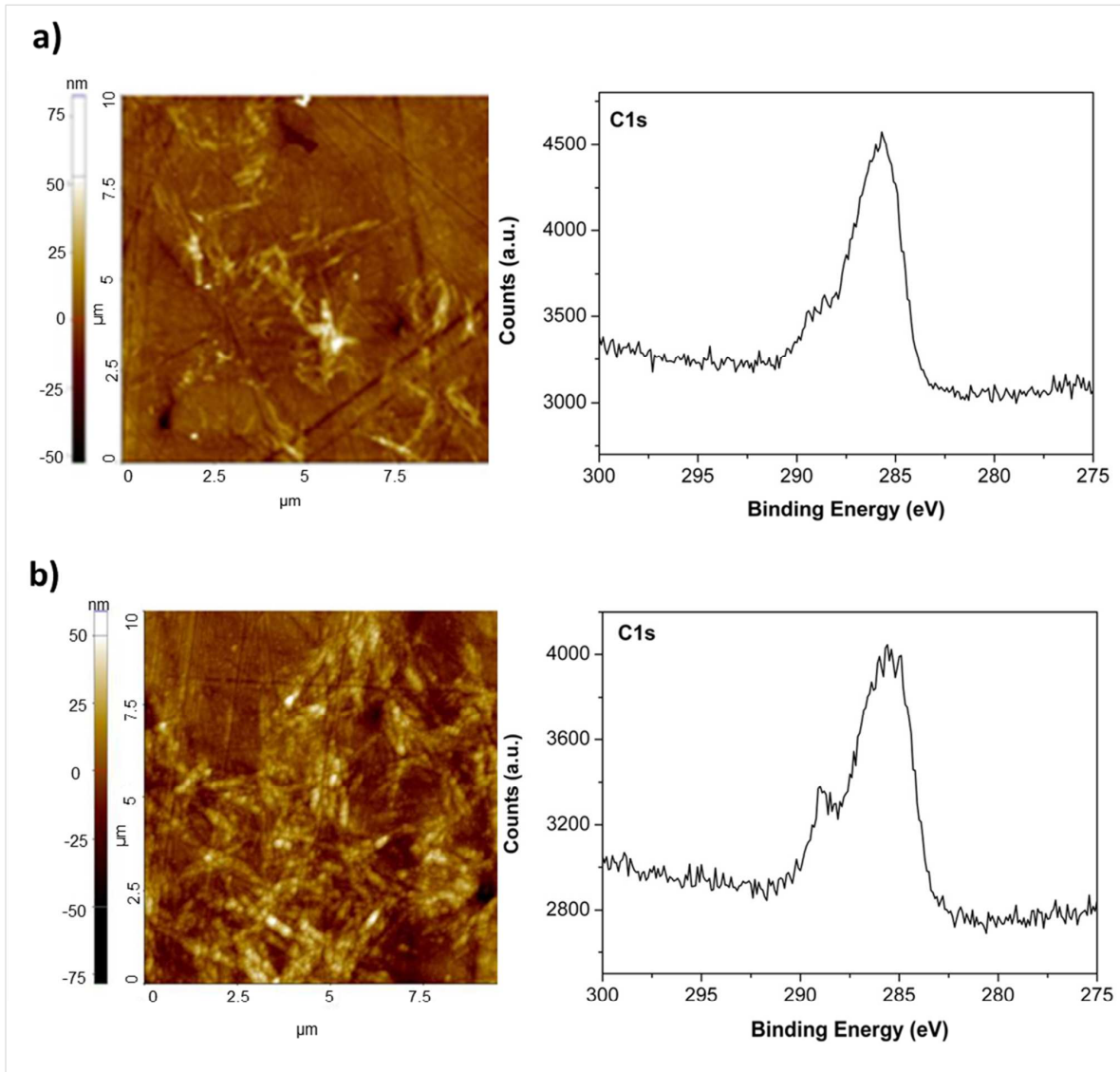


Fig.10 AFM images and XPS C1s signals of Pt/PoAP/VGGVG (A) and Pt/PoAP/BoCVGGVGOEt (B) and after the detection of (VGGVG)₃ fibrils.

Table 1. Curve fitting results of reference XPS spectra reported in Figures 2

Sample	Element	Peak number	BE corr. (eV)	FWH M (eV)	Corrected area (arbitrary unit)	Number of atoms for repeat unit	Assignment
<u>VG VG/Si</u>	C1s	1	285.0	1.66	1763.8	6.0	C (CH)
		2	286.3	1.66	1474.2	5.0	C _α
		3	288.0	1.66	1149.9	3.9	N-C=O
		4	289.0	1.66	410.9	1.4	O-C=O O-C=O*
		5	292.0	1.66	115.1	0.4	CF ₃ *
	N1s	1	400.0	1.90	1337.5	4.5	N-H
		2	401.9	1.90	132.4	0.5	-NH ₃ ⁺
<u>BOC VG VG GOEt/Si</u>	C1s	1	285.0	1.69	2428.8	10.0	C (CH)
		2	286.5	1.69	1696.9	6.9	C _α
		3	288.1	1.69	961.2	3.9	N-C=O
		4	289.5	1.69	480.6	2.0	O-C=O
	N1s	1	400.2	1.98	1214.5	5.0	N-H
<u>(VG VG)_{1.5}/Si</u>	C1s	1	285.0	1.69	1439.10	6.0	C (CH)
		2	286.2	1.69	1202.12	5.0	C _α
		3	287.5	1.69	300.68	1.2	C=O...HOH...O=C
		4	288.4	1.69	936.08	3.9	N-C=O...HN
	O1s	1	531.6	1.64	306.49	1.2	C=O...HOH...O=C
		2	532.3	1.64	946.84	3.9	N-C=O...HN
		3	533.2	1.64	269.37	-	H ₂ O
	N1s	1	400.4	1.89	1202.20	5.0	HN-C=O

Table 2. Curve fitting results of XPS spectra reported in Figures 4, 5 and 9

Sample	Element	Peak number	BE corr. (eV)	FWH M (eV)	Corrected area (arbitrary unit)	At%	Assignment
<u>(VGGVG)₃/aged PoAP</u>	C1s	1	284.8	1.55	7471.56	50.7	C (CH)
		2	285.2	1.55	1288.20	8.7	C _α C-N
		3	286.0	1.55	2768.40	18.8	C-O C=N C-N ⁺
		4	287.2	1.55	1343.04	9.1	C=O
		5	288.7	1.55	1136.64	7.7	COOH
		6	290.3	2.00	373.58	2.5	Shake up
		7	293.1	2.00	373.58	2.5	Shake up
<u>PoAP</u>	C1s	1	284.8	1.55	5435.88	41.4	C arom
		2	285.2	1.55	1864.10	14.2	C-N
		3	286.5	1.55	4256.68	32.4	C-O C=N
		4	288.2	1.55	924.47	7.0	C=O
		5	290.3	2.00	318.92	2.5	Shake up
		6	293.1	2.00	318.92	2.5	Shake up
<u>Aged PoAP</u>	C1s	1	284.8	1.55	4077.56	40.6	C arom
		2	285.2	1.55	1530.68	15.2	C-N
		3	286.5	1.55	2928.41	29.2	C-O C=N
		4	288.4	1.55	1060.87	10.6	C=O
		5	290.3	2.00	218.95	2.2	Shake up
		6	293.1	2.00	218.95	2.2	Shake up
<u>Pt/PoAP/VGGVG</u>	C1s	1	284.8	1.55	8339.24	52.0	C (CH)
		2	286.3	1.55	4773.92	29.7	C-O + C-N + C _α
		3	287.8	1.55	1380.03	8.6	N-C=O C=O+ C=N
		4	289.6	1.55	719.88	4.5	C=O...H ₂ O
		5	291.8	2.00	416.96	2.6	Shake up
		6	293.8	2.00	416.96	2.6	Shake up
	Pt4f	1	71.3	1.45	514.54	57.1	Pt4f _{7/2}
		2	74.6	1.45	385.90	42.9	Pt4f _{5/2}
<u>Pt/PoAP/BoCVGGVG/GOEt</u>	C1s	1	284.8	1.55	5752.24	34.4	C (CH)
		2	285.7	1.55	6693.12	40.0	C-N + C _α
		3	286.9	1.55	2567.25	15.4	C-O + C=O + C=N
		4	288.6	1.55	868.96	5.2	N-C=O
		5	290.0	1.55	265.22	1.6	C=O...H ₂ O
		6	291.8	2.00	287.61	1.7	Shake up
		7	294.6	2.00	287.61	1.7	Shake up
	Pt4f	1	71.1	1.45	270.80	43.2	Pt4f _{7/2}
		2	72.5	1.45	95.46	15.2	PtOx 4f _{7/2}
		3	74.5	1.45	189.68	30.2	Pt4f _{5/2}
		4	76.0	1.45	71.59	11.4	PtOx 4f _{5/2}

FIGURE CAPTIONS

Fig.1 AFM images of VGGVG (a) BocVGGVGOEt (b) and (VGGVG)₃ (c) water suspension (0.1 mg/mL) deposited on silicon wafer.

Fig.2 XPS curve-fitted C1s and N1s spectra of VGGVG (a) BocVGGVGOEt (b) and (VGGVG)₃ (c) water suspension (0.1 mg/mL) deposited on silicon wafer. Curve-fitting results are reported in Table 1. The O1s regions of monomer deposits (2a,2b) are not reported due to the substrate signals interference. Results of the curve-fitted O1s region of the trimer deposits (2c) are reported in Table 1.

Fig.3 Interaction of insulating PoAP with (VGGVG)₃ solution: AFM images and XPS C1s spectra of the PoAP before (on the left) and after (on the right) exposure to (VGGVG)₃ solution.

Fig.4 XPS curve-fitted C1s (a), O1s (b), N1s regions (c) and AFM images 5x5 μm, (d) of insulating PoAP aged 15 days and then exposed for 6 h at 37 °C to the solution of (VGGVG)₃. Curve-fitting results are reported in Table 2.

Fig.5 XPS curve-fitted C1s region of the insulating PoAP analyzed immediately after the electrosynthesis (a) and after 15 days of aging in air at room temperature (b) and relevant AFM images (c,d). Curve-fitting results are reported in Table 2.

Fig.6 XPS C1s spectra and AFM images of the Pt/PoAP electrodes exposed to 15 days aged VGGVG solutions (on the left); XPS C1s spectra and AFM images of the detection of (VGGVG)₃ (on the right).

Fig.7 Interaction of insulating PoAP with BocVGGVGOEt solutions: XPS C1s spectra and AFM images of the Pt/PoAP electrodes exposed to fresh protected-VGGVG solutions (on the left); XPS C1s spectra (on the left) and AFM images (on the right) of the detection of (VGGVG)₃ (on the right).

Fig.8 Cyclic voltammetry of electrosynthesis of insulating PoAP on platinum electrode with a scan rate of 50 mV/s: the first voltammetric cycle (in Black) is registered in 5 mM oAP solution in phosphate buffer (I = 0.1M, pH = 7.0), while the other nineteenth scan are acquired after the

1
2
3
4
5
6
7
8
9
10
11
12
13
14
15
16
17
18
19
20
21
22
23
24
25
26
27
28
29
30
31
32
33
34
35
36
37
38
39
40
41
42
43
44
45
46
47
48
49
50
51
52
53
54
55
56
57
58
59
60

addition of an aqueous solution of VGGVG (A) and BocVGGVGOEt (B) at a concentration of 0.1 mg/mL.

Fig.9 XPS curve fitted C1s and Pt4f regions of PoAP with entrapped VGGVG (A) and BoCVGGVGOEt (B) and relevant AFM images at 10x10 μm magnification. Curve-fitting results are reported in Table 2.

Fig.10 AFM images and XPS C1s signals of Pt/PoAP/VGGVG (A) and Pt/PoAP/BoCVGGVGOEt (B) and after the detection of (VGGVG)₃ fibrils.

Table 1. Curve fitting results of reference XPS spectra reported in Figures 2.

Table 2. Curve fitting results of XPS spectra reported in Figures 4, 5 and 9.

Analytical and Bioanalytical Chemistry

Electronic Supplementary Material

Interactions between elastin-like peptides (ELPs) and insulating poly ortho-aminophenol (PoAP) membrane investigated by AFM and XPS

Maria E. Elvira Carbone^{1*}, Rosanna Ciriello¹, Pasquale Moscarelli², Federica Boraldi², Giuliana Bianco¹, Antonio Guerrieri¹, Brigida Bochicchio¹, Antonietta Pepe¹, Daniela Quaglino², Anna Maria Salvi^{1*}

¹Università degli Studi della Basilicata, Dipartimento di Scienze, DiS, Viale dell'Ateneo Lucano 10, 85100 Potenza, Italy

²Università degli Studi di Modena e Reggio Emilia, Dipartimento di Scienze della Vita, Via Campi 287, 41125 Modena, Italy

Table of Contents

- S1** Interaction of insulating PoAP with VGGVG solutions: XPS C1s spectra (on the left) and AFM images (on the right) of the Pt/PoAP electrodes exposed to fresh (a), 15 days (b) and 76 days (c) aged VGGVG solutions.
- S2** Optical microscope image of the Pt/PoAP foils exposed to solutions of VGGVG 76 days aged (a) and of species present in aged (76 days) VGGVG solution deposited onto silicon substrate (b).
- S3** XPS C1s spectra (on the left) and AFM images (on the right) of the detection of (VGGVG)₃ employing the Pt/PoAP/VGGVG electrodes obtained with fresh (a), 15 days (b) and 76 days (c) aged monomer solutions.
- S4** Interaction of insulating PoAP with BocVGGVGOEt solutions: XPS C1s spectra (on the left) and AFM images (on the right) of the Pt/PoAP electrodes exposed to fresh (a), 15 days (b) and 76 days (c) aged VGGVG solutions.
- S5** XPS C1s spectra (on the left) and AFM images (on the right) of the detection of (VGGVG)₃ employing the Pt/PoAP/BocVGGVGOEt electrodes obtained with fresh (a), 15 days (b) and 76 days (c) aged monomer solutions.
- S6** AFM images of Pt in its pristine state (a) and after interaction with BocVGGVGOEt fresh (b); 15 days (c) and 76 days (d) aged solutions. **The sequence of experiments is to be compared with its analogue in S4.**

Study of PoAP and (VGGVG)₃ interactions, mediated by VGGVG monomers pre-adsorbed on PoAP surfaces from water solutions, differently aged, at ambient conditions: influence of VGGVG terminal groups

H₂-VGGVG-OH

Figures S1 shows the XPS spectra, limited to C1s regions, as the best resolved by curve-fitting of Pt/PoAP surfaces after immersion into VGGVG solutions: a) fresh; b) aged for 15 days; c) aged for 76 days together with the relevant AFM images. By comparing each set with the reference XPS spectra and AFM images of the 'as prepared' electrode, the progressive adsorption of the unprotected monomer on Pt/PoAP by increasing its aging time in water, is confirmed by all evidence, including the attenuation of the underlying platinum substrate, estimated by the parallel decrease of Pt/N ratios, going from 0.84 (fresh) to 0.65 (15days) and 0.44 (76days), see Figures.

Moreover, focusing on details, interesting information are added on the ELP adsorption on PoAP and on its self-aggregation mechanisms. In particular:

- the very limited adsorption of the fresh monomer on Pt/PoAP surface recall the situation previously encountered with the trimer suspension, see Figure 4, where the morphology of the adsorbed layers was not really discernable by AFM;
- the change of C1s peak shape (Fig. S1a), even more remarkable in this case, better suggests that PoAP-ELP interactions have occurred through C=O...H-peptide bonds, as revealed by the carbonyls shifting towards higher BEs (i.e. appearance of carboxylic-like features labeled in Figure 5b) and by the prominent aliphatic component, likely resulting by side chains exposed outward, enhanced by XPS, preventing further adhesion;
- going ahead with ageing time, ELP adsorption progresses and the carbon 1s shape of Pt/PoAP surfaces continues to change accordingly. The carbonyl and carboxyl intensities, ratioed to aliphatic intensity increase with aged ELP, reaching a maximum in 15 days (Fig. S1b). Up to there, the adsorbates, still unstructured but widely distributed, are better detected by AFM, together with light patches here and there over the surface. The augmented ELP coverage (Pt/N=0.65) can be considered as an indication of its aggregation tendency, preannounced as head-tail alignment (Figure 1) of the unprotected sequence, to be evolving over time while ageing in water, presumably, leading to 'longer chain' adsorption on PoAP carrying additional carbonyls, available for further adsorption;
- Finally, the situation after 76 days is very impressive. During the long aging time, the monomer self-aggregation has progressed to a point of producing the amazing supra-molecular structure shown in Figure S1c. However, by comparing the optical images of **Figure S2a** with the optical image of deposits on silicon wafer from the same solution

(**Figure S2b**), it becomes immediately clear that it is the adsorption on Pt/PoAP to specifically promote the assembly of long-aged VGGVG into very long, interconnected, tubular fibres with dimensions of the order of microns, probably facilitated in their propagation by the anchoring mainly offered by carbonyl functionalities over the PoAP surface. The correspondent XPS analysis, shows a higher degree of coverage ($Pt/N=0,45$) and a broad carbon 1s spectra regressed to a shape dominated by aliphatic components, indicative of a nearly saturated coverage, hindering further adsorption.

It was a matter then to see how the three modified electrodes would perform in the presence of the trimer fibrils suspended in water.

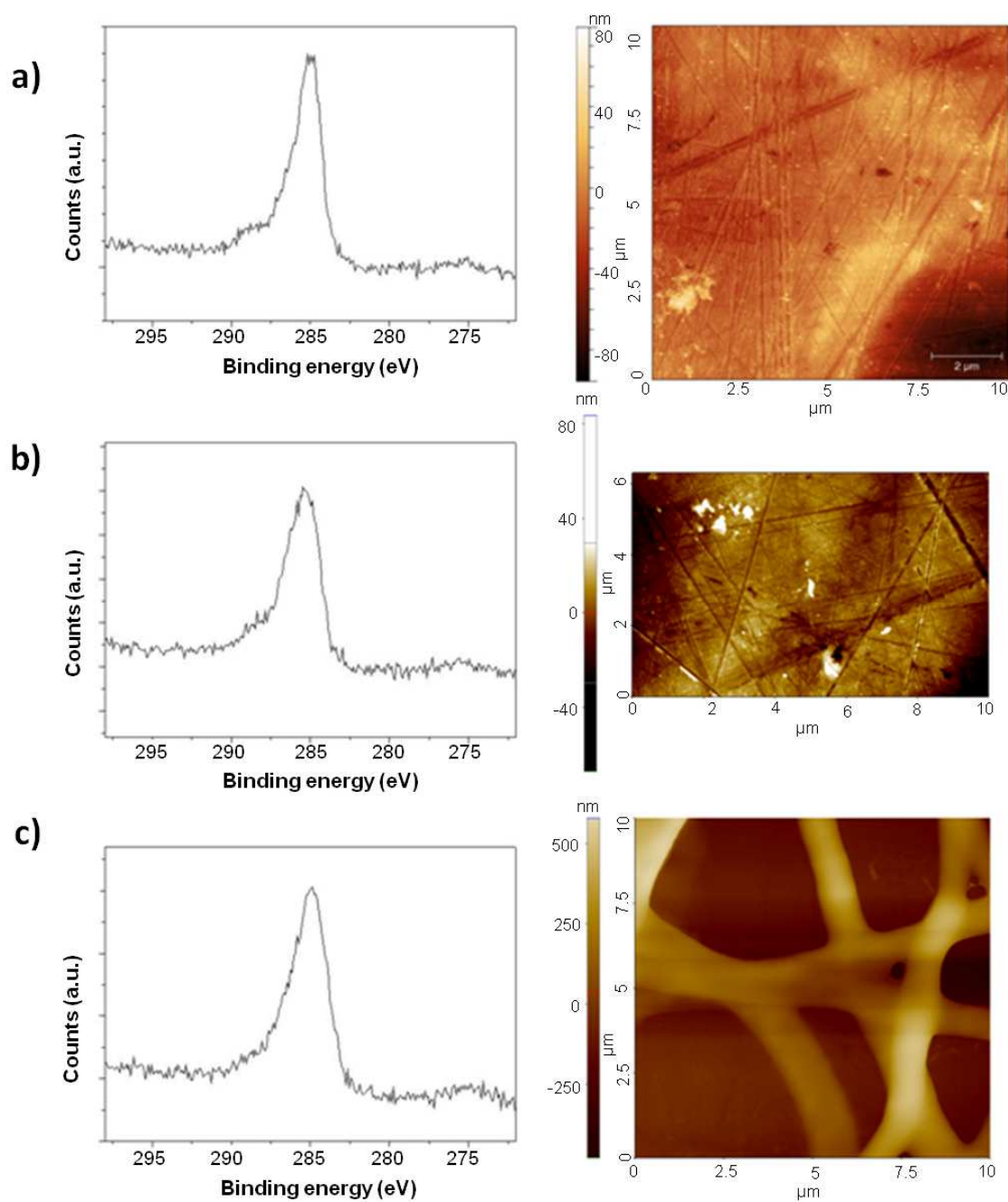
Figures S3 shows the carbon 1s sequences of the three Pt/PoAP/ELP surfaces, after interaction with $(VGGVG)_3$ suspended in water, and the corresponding AFM images. The figures are self-explanatory.

Figure S3a proves, similarly to the precedent 'as prepared' Pt/PoAP electrode of Figure 3, the trimer adsorption on the modified PoAP surface of figure S1a, mainly by XPS. The change of C1s shape testifies that adsorption has taken place to an extent that leaves unaltered the substrate morphology and the Pt/N ratio is roughly the same as before immersion into the trimer suspension.

Figure S3b shows a massive attachment of aggregates also recognizable in previous deposits from trimer suspension imaged on silicon. This time, the trimer adsorption masks the underneath features, in parallel, XPS gives the ratio Pt/N reduced to 0.47, index of greater coverage in comparison to the reference surface of figure S1b.

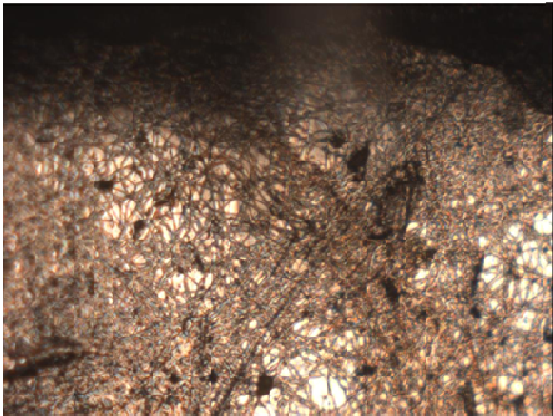
In Figure S3c the magnified AFM image shows a kind of deterioration of the, previously intact, interconnected fibres of figure S1c while XPS shows a further narrowing of C1s peak around the aliphatic component. Taken with cautions, given the massive envelope of fibers, results from curve-fitting indicate the same Pt/N ratio as before, as if no trimer attachment has taken place. In reality, it could be that further interactions with the suspended trimer, inducing the deterioration of fibres, also leads to a concomitant detachment of some, less bounded, parts of their extended envelope.

In order to complete this study and find the best Pt/PoAP/ELP combination for sensing amyloid fibrils, the same set of experiments was repeated with the same ELP sequence protected with terminal groups, as reported in the following paragraph.

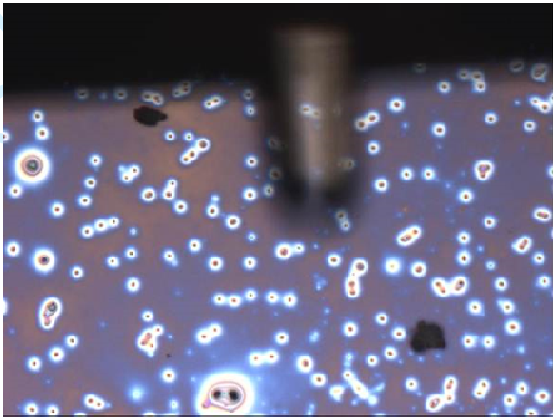


S1 Interaction of insulating PoAP with VGGVG solutions: XPS C1s spectra (on the left) and AFM images (on the right) of the Pt/PoAP electrodes exposed to fresh (a), 15 days (b) and 76 days (c) aged VGGVG solutions.

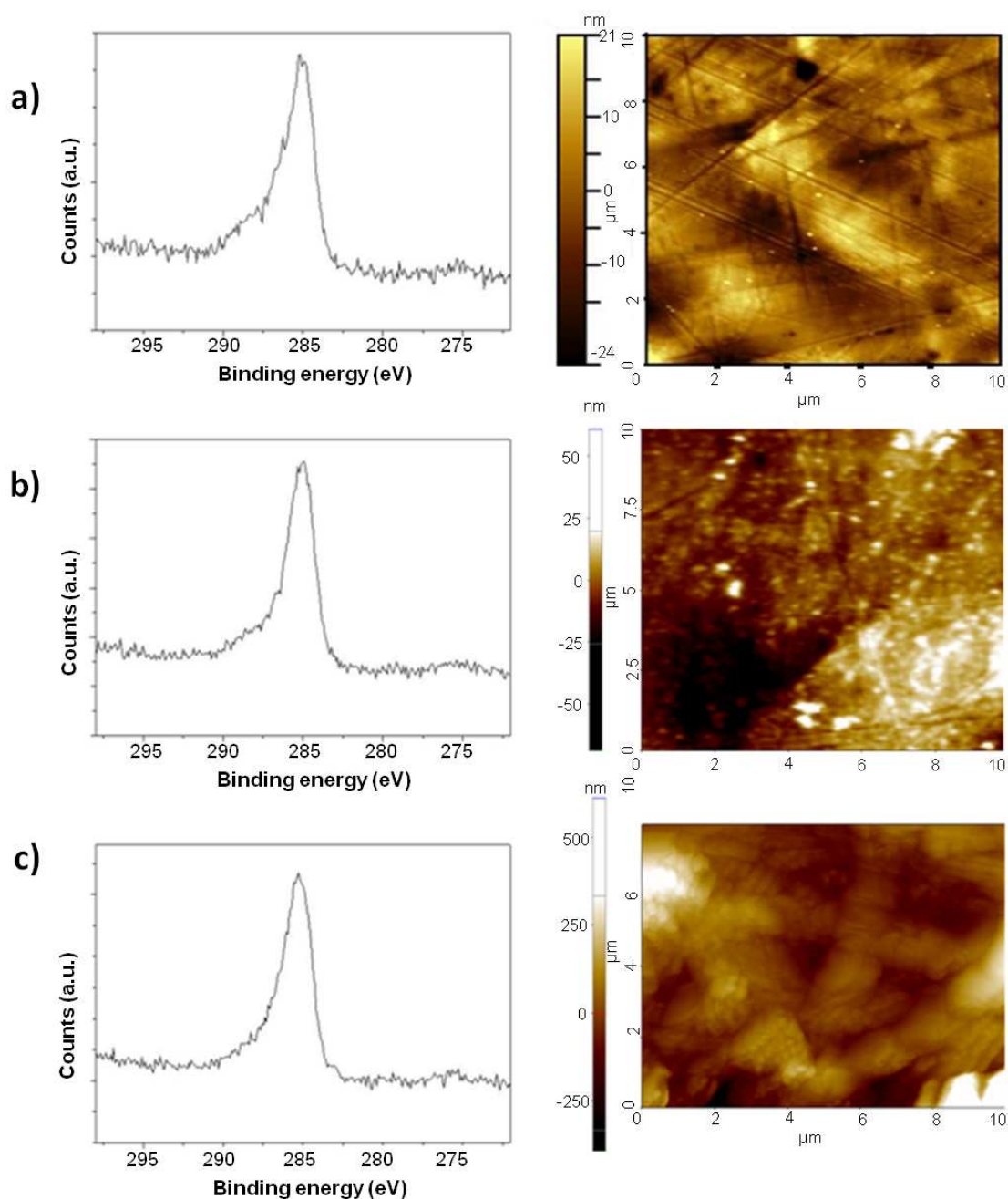
a)



b)



S2 Optical microscope image of the Pt/PoAP foils exposed to solutions of VGGVG 76 days aged (a) and of species present in aged (76 days) VGGVG solution deposited onto silicon substrate (b).



S3 XPS C1s spectra (on the left) and AFM images (on the right) of the detection of (VGGVG)₃ employing the Pt/PoAP/VGGVG electrodes obtained with fresh (a), 15 days (b) and 76 days (c) aged monomer solutions.

BoC-VGGVG-OEt

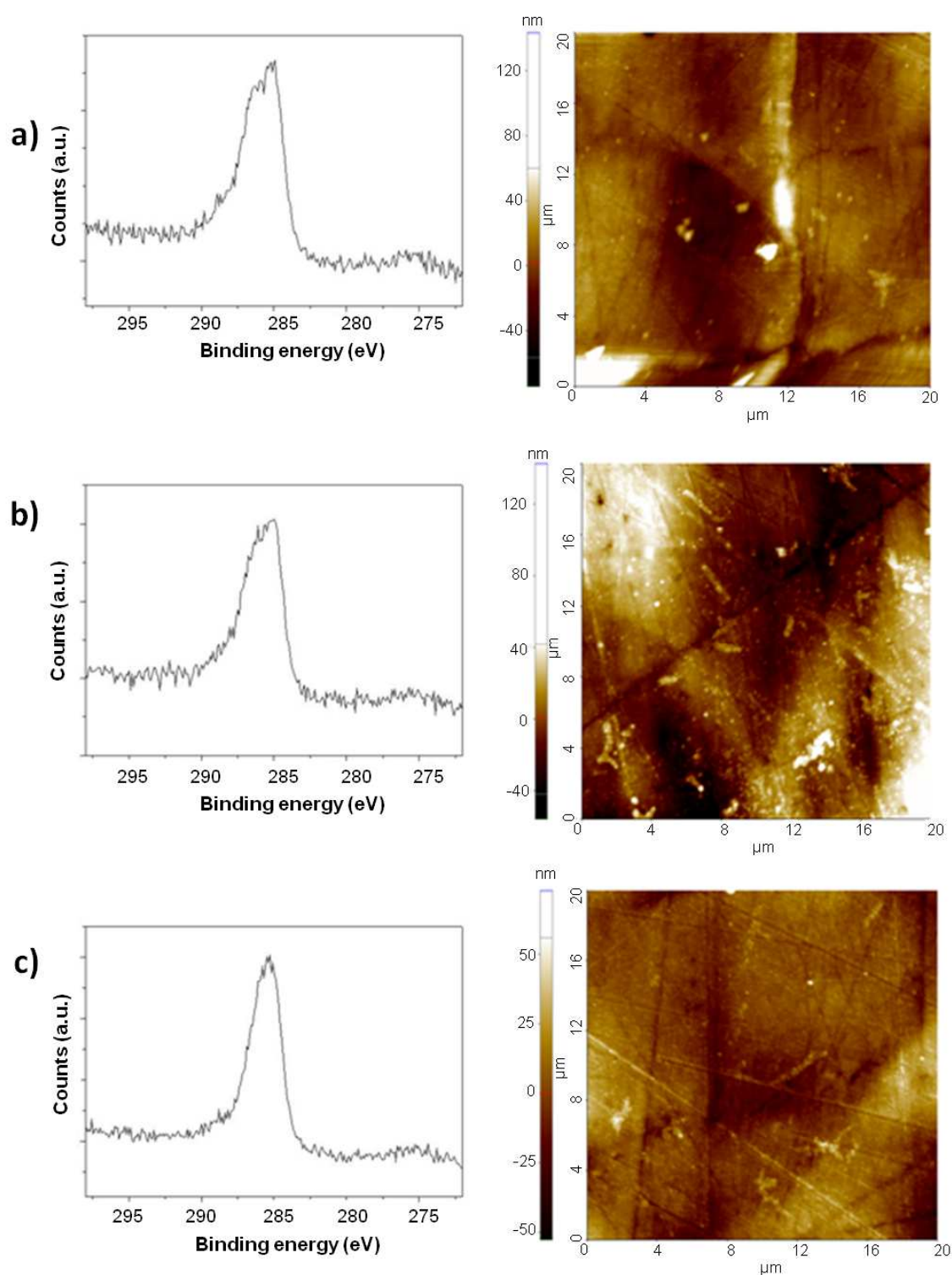
Figures **S4** and **S5** are resuming the same experiments with BoC-VGGVG-OEt, using the same experimental conditions, carried out for the unprotected pentapeptide.

Briefly, the two set of figures compare, by XPS and AFM, the Pt/PoAP surface modified by BoC-VGGVG-OEt adsorption from fresh (a), aged for 15 days (b) and long aged for 76 days (c) solutions, before (Figure 10) and after (Figure 11) interaction with the aged trimer suspension.

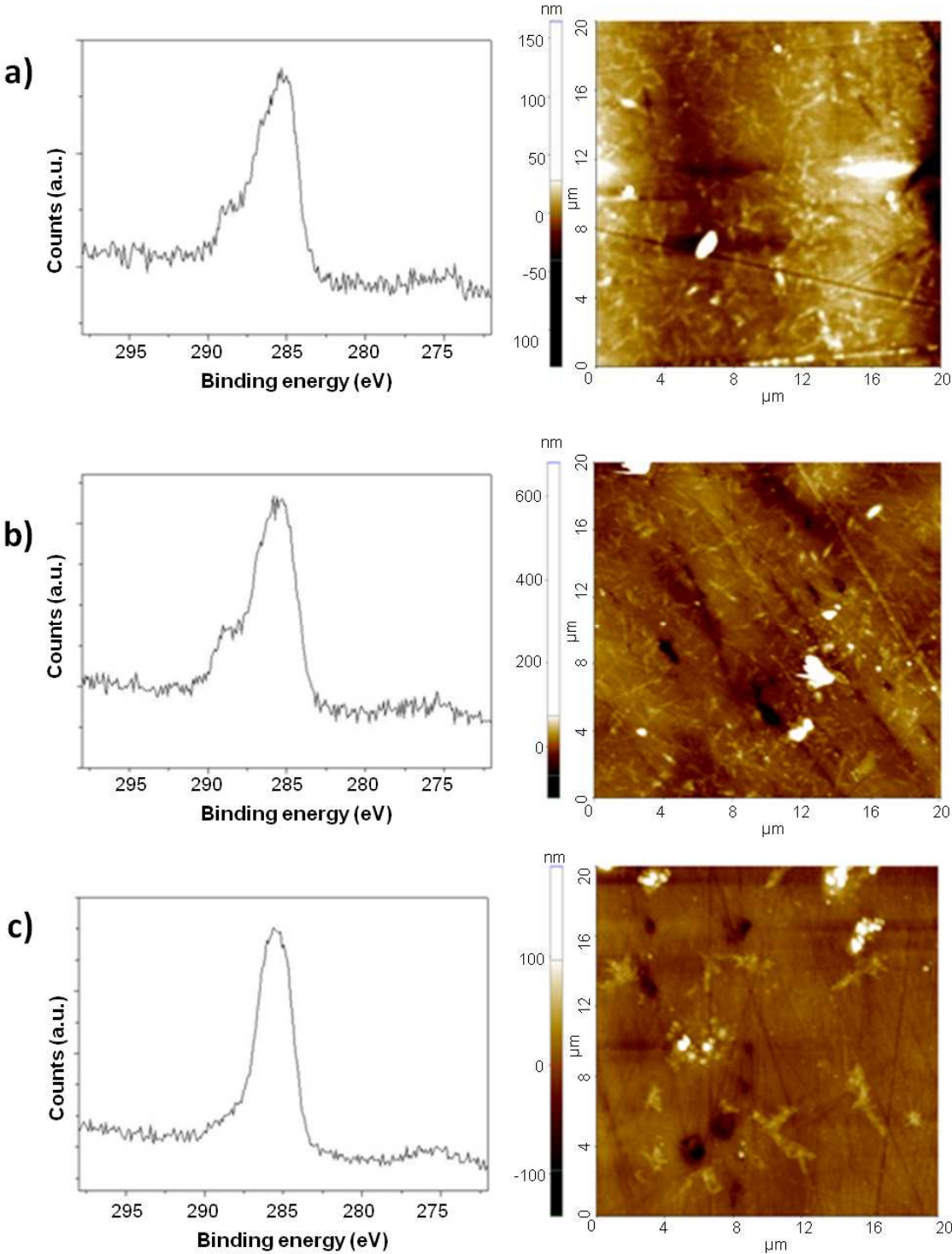
Going through the series, some similarities with the unprotected monomer are seen and regard the effect of ageing time, deducible also for the protected monomer by the correlation between the coverage degree of PoAP surfaces and changes of the C1s peak shape, either before and after trimer adsorption. However, the differences emerged are more important to deepen the understanding of the 'interaction' mechanisms under study, as hereafter discussed.

The first important 'difference' regards the PoAP-monomer interactions, in this case, mainly involving the aromatic repeat and the encumbering aliphatic terminal groups, respectively. In fact, limiting the analysis to the fresh and short-aged BoC-VGGVG-OEt solution, (leaving out long aged conditioning, as promoter of massive adsorption leading to coverage saturation even prone to detachment), it is easily noticed that C1s peak shapes of Figures S4a,b differ from the correspondent in Figures S1a,b of the unprotected monomer. In this case, particularly for the fresh solution, the oxygenated functionalities are those exposed outwards, thus oppositely to the its homologue, the protected monomer interacts with PoAP by means of hydrophobic forces.

Another important and consequent difference is shown along the series of Figures S5 where signs of the trimer adsorption are clearly identified already for the Pt/PoAP surface modified with BoC-VGGVG-OEt from fresh solution (Fig. S5a). Indeed AFM and XPS respectively show aggregate features and C1s peak shape resembling those reported in Figure 3, related to trimer deposits on silicon wafer from the same water suspension. Thus, pre-adsorption of the protected monomer on PoAP, both freshly prepared without any need of further ageing, occurs via hydrophobic forces, while the remaining groups prone to H-bonds make the outer surface very sensitive towards trimer fibrils.

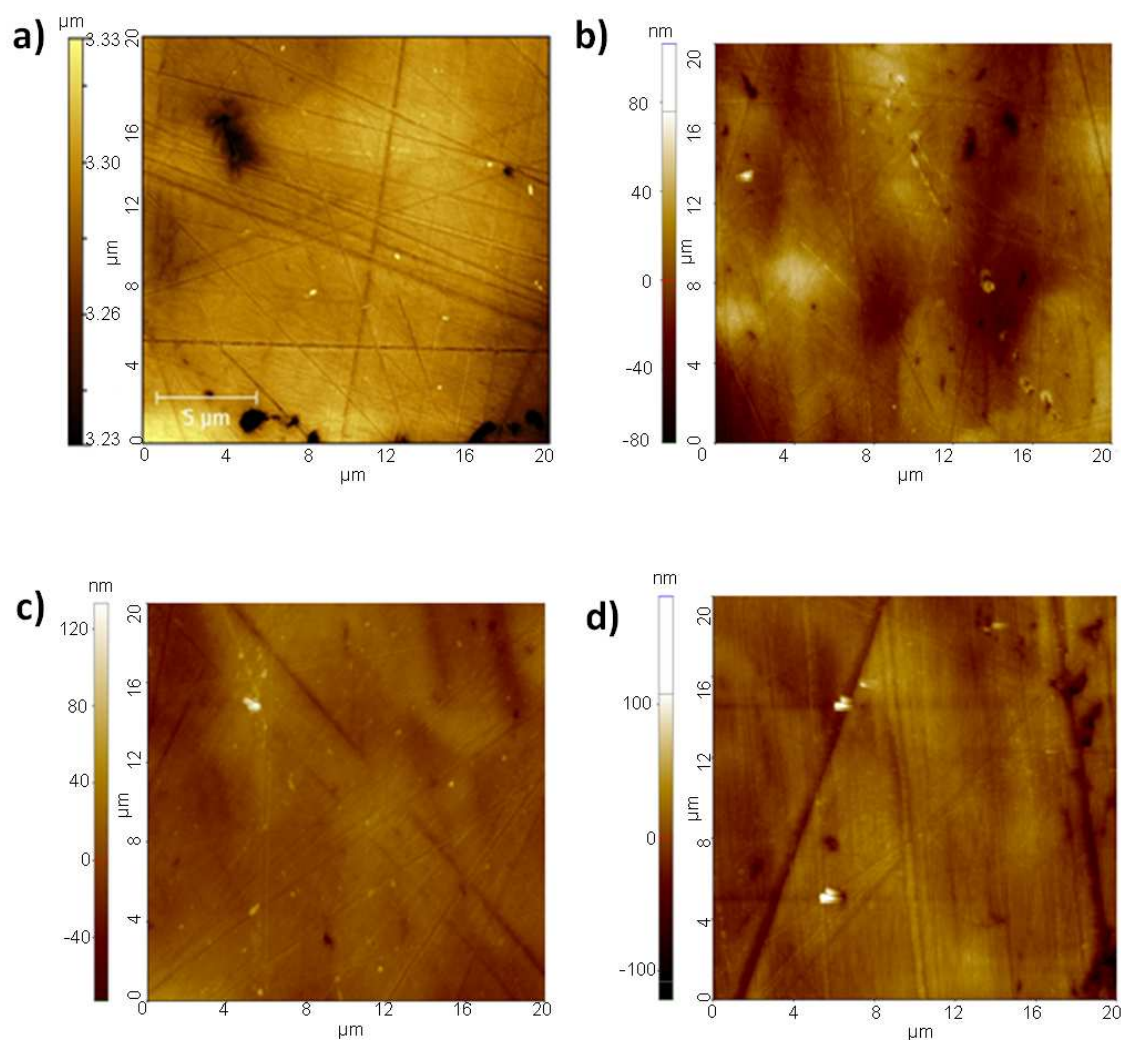


S4 Interaction of insulating PoAP with BocVGGVGOEt solutions: XPS C1s spectra (on the left) and AFM images (on the right) of the Pt/PoAP electrodes exposed to fresh (a), 15 days (b) and 76 days (c) aged VGGVG solutions.



S5 XPS C1s spectra (on the left) and AFM images (on the right) of the detection of (VGGVG)₃ employing the Pt/PoAP/BocVGGVGOEt electrodes obtained with fresh (a), 15 days (b) and 76 days (c) aged monomer solutions.

Role of Platinum substrate



S6 AFM images of Pt in its pristine state (a) and after interaction with BocVGGVGOEt fresh (b); 15 days (c) and 76 days (d) aged solutions. **The sequence of experiments is to be compared with its analogue in S4.**